EFFECTS OF PUBERTAL HIGH FAT DIET AND OVERWEIGHT ON MAMMARY TUMORIGENESIS IN FVB AND BALB/C MICE

By

Yirong Zhu

A DISSERTATION

Submitted to
Michigan State University
in partial fulfillment of the requirements
for the degree of

Cell and Molecular Biology — Doctor of Philosophy

2016

ABSTRACT

EFFECTS OF PUBERTAL HIGH FAT DIET AND OVERWEIGHT
ON MAMMARY TUMORIGENESIS IN FVB AND BALB/C MICE

By

Yirong Zhu

High animal fat diet (HFD) has long been suspected to increase breast cancer risk. Studies in human and rodents support the hypothesis that environmental exposure in puberty will affect breast cancer risk in adulthood. This study examined the effects of pubertal HFD in both obesity-prone FVB mice and obesity-resistant BALB/c mice. FVB mice were fed a high fat diet from three weeks of age and exposed to DMBA-induced carcinogenesis. The pubertally initiated HFD increased mammary tumor incidence, showed a trend toward recruitment of an increased number of macrophages to early hyperplastic lesions, and had no effects on proliferation or angiogenesis in FVB mice. Wild type BALB/c mice were transplanted with *Trp53*-null mammary epithelium. HFD restricted to puberty increased early tumor incidence over a 52-week time course, but not over a longer period. Life-long and adult HFD increased tumor incidence over a 70-week time course. Notably, adult HFD specifically increased the incidence of spindle cell carcinomas that resemble claudin-low, triple negative human breast cancer. Irrespective of histopathology, tumors that developed in mice fed life-long HFD, pubertal HFD, and adult HFD all showed enhanced tumor proliferation, angiogenesis and M2-type macrophage recruitment. HFD promotes mammary tumorigenesis independent of obesity. In addition to puberty, there may be multiple windows of susceptibility to HFD.

To Zaoli,
My light and inspiration

ACKNOWLEDGMENTS

My very sincere gratitude goes to my mentors Dr. Sandra Haslam and Dr. Richard Schwartz. As mentors, Dr. Haslam and Dr. Schwartz shared with me their expertise in scientific inquiries and led through examples of scholarship and productivity. Their passion and dedication for breast cancer research continuously fueled my development as a scientist. I am deeply grateful for the flexible and encouraging environment they created that allowed me to think innovatively and grow intellectually. Their critical guidance is invaluable for the timely completion of this dissertation.

I am also thankful for my dissertation committee, Dr. Kathleen Gallo, Dr. Karl Olson and Dr. Chengfeng Yang, for their incredible knowledge, insight and encouragement.

I thank Dr. Justin McCormick and Bethany Heinlen, who have been my tremendous advocates, and created many opportunities for me to broaden my professional development. I thank Phyllis K. and Walter P. Dell for their generosity in establishing the scholarship fund that supported my work here at Michigan State University.

I am very much indebted to Dr. Yong Zhao and Ying Siow (May) Tan, who initiated the animal studies of high fat diet in the p53-null mammary transplant model, and laid the solid foundation for my dissertation work. I am thankful for Dr.

Mark Aupperlee and Jessica Bennett for their technical knowledge and assistance. I also thank Yousef Seyam for his diligent assistance in animal care.

I thank my wife, Zaoli Zhang for her endless love and support. At many moments of failure and moments of despair, she reminds me of the important things in life. She has a special ability to take my fear away, so I could find new ways to solve the problems at hand. At those precious moments of success and milestones, she shared my joy and gave me purpose. My work would not have been possible without her sacrifice, and I appreciate the service of Megabus and Amtrak that closed the distance between us.

I thank my parents, Min Zhu and Sudong Jiang, for giving me an inquisitive mind, and encouraging my decision to pursue the wonders of life thousands of miles away from them. They may not always comprehend, but they always listen to me combing through my ideas, in science and in life.

Last but not least, I dedicate my work to my grandmother, Xiulan Wei. She was diagnosed with metastatic cancer and passed away while I worked to further the understandings of cancer. She gave me motivation to the grinding day-to-day work, and her fighting spirit gave me hope in our struggle to combat cancer.

TABLE OF CONTENTS

LIST OF TABLES

LIST OF FIGURES

KEY TO ABBREVIATIONS

Ab, antibody;

AhR, aryl hydrocarbon receptor;

ANOVA, analysis of variance;

Arb., arbitrary;

Arg1, arginase 1;

BALB/c, Bagg albino c;

BMI, body mass index;

Bmp7, bone morphogenetic protein 7;

BrdU, 5-bromo-2'-deoxyuridine;

c-Myc, avian myelocytomatosis virus oncogene cellular homolog;

C57BL/6, C57 black 6;

Cat., catalog;

Ccdn2, cyclin D2;

CCR2, C-C chemokine receptor type 2;

CD, cluster of differentiation;

Cdk, cyclin-dependent kinase;

CI, confidence interval;

CL, claudin-low;

CSF-1, colony stimulating factor 1;

Cy5, cyanine 5;

DAPI, 4', 6-diamidino-2-phenylindole;

DD1α, pro-apoptotic death domain 1alpha;

DMBA, 7, 12-dimethylbenz[a]anthracene;

EDTA, ethylenediaminetetraacetic acid;

ELISA, enzyme-linked immunosorbent assay;

EMT, epithelial-to-mesenchymal;

EPIC, the European investigation into cancer and nutrition study;

ER, estrogen receptor;

FVB, friend virus B-type;

GEO, gene expression omnibus;

GH, growth hormone;

GH-R, growth hormone receptor;

Gm11937, predicted gene 11937;

Gpr75, G Protein-Coupled Receptor 75

H&E, hematoxylin and eosin;

HER2, human epidermal growth factor receptor 2;

HFD, high saturated animal fat diet;

IFNa, interferon alpha;

Igf-1r, Insulin-like growth factor 1 receptor;

IGF-I, insulin-like growth factor I;

IL, interleukin;

Inha, inhibin alpha;

K18, cytokeratin-18;

K5, cytokeratin-5;

LFD, low fat diet;

M-CSF, macrophage colony-stimulating factor;

M-CSFR, macrophage colony-stimulating factor receptor;

MCP-1, monocyte chemoattractant protein-1;

MMTV, mouse mammary tumor virus;

mTOR, mammalian target of rapamycin;

NF-kB, nuclear factor-kB;

NHS II, the nurses' health study II;

NK, natural killer;

Olfr10, olfactory receptor 10;

PCNA, proliferating cell nuclear antigen;

Phc1, polyhomeotic homolog 1;

PND, post-natal day;

PR, progesterone receptor;

PRC1, polycomb-group repressive complex 1;

PRLR, prolactin receptor;

qPCR, quantitative polymerase chain reaction;

RANKL, receptor activator of NF-kB ligand;

Ras, rat sarcoma viral oncogene homolog;

Rb, retinoblastoma;

RR, relative risk;

RT, room temperature;

SD, standard deviation;

SEM, standard error of the mean;

Smad2, mothers against decapentaplegic homolog 2;

Sst, somatostatin receptor;

Tag, large T antigen;

TEB, terminal end bud;

TGF, transforming growth factor;

TLR, toll-like receptor;

Tnfsf11, tumor necrosis factor ligand superfamily member 11;

TOB, transducer of ErbB-2;

Trp53, transformation-related protein 53;

TUNEL, terminal deoxynucleotidyl transferase dUTP nick end labeling;

WHIDM, the women's health initiative dietary modification trial;

Wnt, wingless-type MMTV integration site.

CHAPTER 1

Introduction

The American Cancer Society estimates more than 230, 000 cases of breast cancer will be diagnosed in the US in 2015 [1]. If the current incidence rate remains unchanged, 1 in 8 women born in the US today who live to her 80s will be diagnosed with breast cancer sometime during her life [2]. There are marked variations in breast cancer risk by race and ethnicity. It is known that women who migrate from countries with lower breast cancer rates acquire the higher risk of the new country [3, 4]. Evidence from multiple migration studies supports the acculturation-transition model and points towards potential environmental and behavioral determinants of breast cancer risk [5-7]. Furthermore, meta-analysis identified early migration in the first two decades of life and generation in the host country to be particularly important in acquiring the increased breast cancer risk [8]. While almost all migration studies focused on populations moving from lower risk countries to industrialized ones, a small study in Zimbabwe found the increased risk in the European migrants remained elevated despite long-term residence, suggesting the risk rendered from early life environment may not be reversible [9].

Dietary acculturation has been hypothesized to contribute to the increased breast cancer risk in Western countries [3, 10, 11]. However, epidemiological studies of diet and breast cancer in human populations vary significantly in the definition of dietary patterns and the results are largely inconsistent [12]. A typical definition of the Western diet consists of higher consumption of processed and red

meats, refined grains, fried food, sweets, soft drinks, and lower consumption of fruits and vegetables [12]. In a recent review of 24 cohort and case-control studies by Albuquerque *et al.* [12], 8 reported a positive correlation between the Western diet and breast cancer, 15 found no associations, and one reported an inverse association. Specific components of the Western diet have been investigated. Expert opinions from the Continuous Update Project on the association of red and processed meat consumption, total caloric intake, and/or total fat intake with breast cancer risk remain inconclusive [13]. Many case-control studies identified positive links between fat intake and risk of breast cancer, but recent meta-analysis and pooled analysis of cohort studies failed to support these associations [14]. Compared to case control studies, prospective dietary data in the cohort studies are advantageous in avoiding recall bias and allowing for error corrections from repeated measurements. To further examine the potential link between dietary fat intake and breast cancer risk, the Women's Health Initiative Dietary Modification (WHIDM) randomized controlled trial recruited post-menopausal women to test a low fat diet (LFD, <20% energy) intervention for prevention of breast cancer [15]. During the intervention period of 8 years on average, women with the highest baseline dietary fat intake (>37% energy) had a reduced risk for invasive breast cancer. The protective effects were not carried forward after the intervention period; there was no risk reduction observed during the additional 5 years of post-intervention follow-up [15]. Weight loss and post-intervention weight gain were identified as potential confounders. The trial was further limited by the fact that the intervention group had lower fat intake, but did not reach the goal of <20% energy

from fat. A greater number of individuals who under-reported their total energy intake were also observed in the intervention group. The role of high fat diet (HFD) in the etiology of breast cancer may also be subtype dependent. A recent analysis from the European Investigation into Cancer and Nutrition (EPIC) study, a prospective cohort study [16], evaluated fat intake and subtypes of breast cancer, and reported high total and saturated fat intake to increase the risk of estrogen receptor positive (ER+) and/or progesterone receptor positive (PR+) breast cancer, but not the receptor negative diseases.

The majority of the observational studies and the WHIDM trial focused on habitual diet in adulthood. However, emerging evidence suggests that the timing of the dietary assessment may be critical in evaluating its contribution to breast cancer risk. A recent update on the prospective cohort study, Nurses' Health Study II (NHS II), during 20-years of follow-up identified a positive association of higher intake of red meat and animal fat in adolescence and early adulthood with risk of premenopausal breast cancer [17, 18]. In the same cohort, saturated fat, but not total fat intake, in early adulthood was also found to be associated with increased breast cancer risk in all women. Women who consume a high fat diet are frequently overweight or obese. Strikingly, the increase in breast cancer risk by high animal and saturated fat was only significant in normal weight women [17, 19]. Obesity itself has been identified to be a risk factor for post-menopausal breast cancer, and meta-analyses reported a pooled relative risk of 1.12 (95% CI = 1.08-1.16 , $p<0.0001$) for every 5kg/m^2 increase in body mass index (BMI) [20]. However, for pre-menopausal breast cancer, obesity is associated with a decreased risk (pooled

RR = 0.92, 95% CI = 0.88-0.97, p=0.04) [20]. The results from the NHS II, however, suggest the high fat diet itself rather than weight gain is responsible for the increased risk. These findings also highlight the lasting effects of a high fat diet in conferring breast cancer risk and support the idea that puberty and early adulthood is a window of susceptibility.

The pubertal mammary gland undergoes rapid cellular proliferation [21]. Ample evidence supports the conclusion that the pubertal mammary gland is highly sensitive to radiation-induced carcinogenesis [22]. Furthermore, in preclinical rodent models, the carcinogen must be administered during the period of puberty to produce significant mammary tumors [23]. A HFD can alter mammary gland pubertal developmental programs. In obesity-prone C57BL/6 mice, HFD inhibits pubertal development with decreased epithelial proliferation and stunted ductal elongation. In contrast, pubertal mammary development is accelerated in obesity-resistant BALB/c mice [24]. In mouse mammary tumor models, pubertally initiated HFD consistently enhanced tumorigenesis in diverse genetic backgrounds with varying degrees of weight gain [25-28]. Genetically engineered mice with elevated endogenous GH/IGF-I in a C57BL/6 background with increased endogenous GH showed increased tumor incidence only in HFD-fed mice [25]. HFD was reported to shorten tumor latency in a carcinogen-induced model using 7, 12-dimethylbenz(a)anthracene (DMBA) in BALB/c mice [26]. MMTV-neu mice in the FVB background on HFD had earlier onset of a second tumor and a twofold greater incidence of the second tumor [27]. HFD stimulated growth of injected 4T1 mouse

mammary tumor cells in BALB/c mammary fat pads, and promoted liver and lung metastases [28].

Study design in mouse models of HFD and breast cancer vary in methods of tumor initiation, diet compositions, timing and duration of the diet, and genetic background of mouse strain, all of which need to be taken into consideration to understand mammary biology and how each model simulates human mammary development and tumorigenesis. I sought to expand on the work of Zhao *et al.* [26] in obesity-resistant BALB/c mice and a preclinical model of premenopausal breast cancer, and to further elucidate and differentiate the effects of HFD and obesity on the development of mammary tumors, allowing for more robust comparisons. To that end, in Chapter 2, I tested the hypothesis that in obesity-prone FVB mice, independent of weight gain, a pubertally initiated HFD would accelerate pubertal mammary ductal elongation by enhancing epithelial proliferation. I also hypothesize that a pubertally initiated HFD would increase the incidence and shorten the latency of DMBA-induced tumorigenesis.

In concordance with epidemiological data, work from our lab suggests that a HFD restricted to puberty is sufficient and required for promoting DMBA-induced tumors in normal weight BALB/c mice [29]. However, in several other mouse strains and tumor models, an adult-initiated HFD from 10 weeks of age was also found to be sufficient to promote mammary tumorigenesis. In the MMTV-TGFα model on the C57BL/6 background, some mice fed a moderate HFD remained in the weight range of a chow-fed control. All HFD-fed mice developed tumors with

shortened latency, and the most obese group had the shortest tumor latency [30]. Also in the obesity-prone C57BL/6 background, HFD decreased MMTV-Wnt-1 tumor latency and resulted in more poorly differentiated tumors expressing mesenchymal makers [31]. HFD-fed FVB C3(1)-Tag mice had decreased tumor latency compared to LFD controls in either nulliparous or parous mice [32, 33]. However, few studies of adult HFD were performed in normal weight BALB/c mice. Thus, it remains to be investigated whether the pubertal window of vulnerability is unique to a carcinogen-induced model in BALB/c mice. In Chapter 3, I tested the hypothesis that the pubertal HFD is more broadly sufficient and required for enhanced tumorigenesis in the *Trp53*$^{-/-}$ mammary transplant tumor model in the BALB/c background. Tumor suppressor *Trp53* is one of the most mutated genes in breast cancer [34], and *Trp53*$^{-/-}$ mammary transplants have an extended tumor latency which allows for evaluation of the long-term consequences of a pubertal HFD on tumorigenesis [35].

Finally, in Chapter 4, I compare and contrast our findings from the FVB DMBA model and the BALB/c *Trp53*$^{-/-}$ transplant model. I discuss future directions in understanding the effects of HFD on mammary tumorigenesis, and remaining challenges in translation to medical practice.

CHAPTER 2

Effects of Pubertal High Fat Diet and Weight Gain On Mammary Tumorigenesis in Obesity-Prone FVB Mice

Introduction

Many case-control studies identified positive associations between fat intake and risk of breast cancer, but recent meta-analysis and pooled analysis of cohort studies failed to support these associations [14]. The majority of the observational studies focus on diet in adulthood at the time of breast cancer diagnosis [14]. However, emerging evidence suggests that the timing of the dietary assessment may be critical in evaluating its contribution to breast cancer risk [36]. Consumption of a high fat diet is also associated with increased BMI and obesity [37]. Therefore, distinguishing between the effects of diet composition vs. weight gain/obesity is challenging. A recent update on the prospective cohort study, Nurses' Health Study II (NHS II), during 20-years of follow-up identified a positive association of higher intake of red meat and animal fat in adolescence and early adulthood with risk of premenopausal breast cancer [17-19]. In the same cohort, saturated fat, but not total fat intake, in early adulthood was also found to be associated with increased breast cancer risk in all women. Strikingly, the increase in breast cancer risk by high animal and saturated fat was only significant in normal weight women [17-19]. These latter findings are in accord with our recent findings in a preclinical model that a diet high in saturated animal fat (HFD), initiated during the puberty in obesity

resistant BALB/c mice, promotes carcinogen-induced mammary cancer development [26].

Obesity has been implicated in increased breast cancer risk, specifically in premenopausal African American women and more generally in postmenopausal women overall [38, 39]. Childhood obesity has more than doubled in children and tripled in adolescents in the past 40 years [40]. Alteration of future breast cancer risk is at the forefront of suspected health impacts from childhood obesity, partly because puberty is a time of rapid breast development and likely a particularly sensitive period for environmental exposures [41, 42]. The effect of increased body weight induced by adult HFD has been reported to increase mammary tumorigenesis in mice in various transgenic oncogene-induced models [43, 44]. However, the effect of HFD-induced pubertal obesity and mammary cancer susceptibility is less well known. To address this question we investigated the effects of HFD initiated in peripuberty on carcinogen-induced mammary tumorigenesis in the FVB mouse strain, which have been reported to gain weight on HFD [45].

Material and Methods

Mice and diet

Three-week-old female FVB mice were purchased from Charles River (Kingston, NY). After 1 day of acclimatization, they were assigned to either a low fat diet (LFD) or a high fat diet (HFD). The LFD (Research Diets D11012202) has 10%

calories from fat, 70% from carbohydrates and 20% from protein. The HFD (Research Diets D11012204) has 60% calories from fat, 20% from carbohydrates and 20% from protein. The additional source of fat in the HFD comes from lard (Table 2.1). Mice were maintained on their respective diets until the end of the experiments. Food and water were provided *ad libitum*, and mice were housed in standard facilities with a 12:12h light-dark cycle. Body weight was measured twice weekly. Sexual maturity was monitored by daily observation for vaginal opening between post-natal day (PND) 25 and PND35. For assessment of peripubertal effects of diet, time course studies were carried out; at each time point 5 mice were sacrificed after 1, 2, 3, or 4 weeks on diet. All mice were sacrificed at estrus stage, when vaginal smear showed a predominance of cornified epithelial cells. 5-Bromo-2′-deoxyuridine (BrdU, 70 μg/g body weight; Sigma-Aldrich) was administered via intraperitoneal injection two hours prior to sacrifice. Plasma was obtained via cardiac puncture. All animal protocols were reviewed and approved by the Institutional Animal Care and Use Committee at Michigan State University.

Tumorigenesis

Using ovary-intact mice up to 1 year of age represents a preclinical model of premenopausal breast cancer. Three-week-old mice were randomly assigned to the LFD or HFD group (LFD n=60, HFD n=80). Beginning at 5 weeks of age, mice in both groups were treated once a week for four weeks with DMBA dissolved in vegetable oil via oral gavage (50 mg/kg body weight/mouse). At 13 weeks of age (i.e., after 10 weeks on diet) and at 19 weeks of age (i.e., after 16 weeks on diet), 5 mice from each

group were randomly selected and sacrificed at estrus stage to examine the early effects of HFD prior to the development of palpable tumors. The remaining mice were palpated twice weekly for tumor development until they reached 57 weeks of age, 1 year after initial DMBA treatment. Tumors were harvested when they reached 1cm in diameter. Two hours prior to sacrifice, mice were injected with BrdU. Portions of the tumor were formalin fixed and either processed as whole mounts [46] or paraffin-embedded for hematoxylin and eosin (H&E) staining and immunohistochemistry [47]. Whole mount preparations of glands and H&E sections were scored for overall morphology, the presence of hyperplasia, and neoplasia [48]. All lesions and tumors were reviewed and classified, as previously described [49]. The remaining portions were snap frozen for RNA extraction.

Whole mount analysis

Formalin-fixed inguinal mammary glands were prepared for whole mount analysis as previously described [26]. For assessment of pubertal development, longitudinal growth was measured by the distance between the most distal terminal duct and the lymph node. Terminal end buds (TEBs) were defined as enlarged multilayered ductal tips with a diameter greater than 100 μm that were surrounded by adipocytes and located in the periphery of the gland.

Immunohistochemistry

BrdU was detected using mouse monoclonal antibody (1:100; Cat #: RPN202; GE Healthcare, Little Chalfont, Buckinghamshire, UK) with incubation at RT for 2

hours followed by Alexa 488–labeled goat anti-mouse secondary Ab (1:200; Invitrogen Molecular Probes, Grand Island, NY). CD31 was detected with rabbit polyclonal anti-CD31 (1:50; Cat #: AP15436PU-N, Acris Antibodies, Inc., San Diego, CA) with incubation at RT for 2 hours followed by secondary swine anti-rabbit Ab (DAKO, Carpinteria, CA), and ABC reagent (Cat #: PK-7100; Vector Laboratories, Inc., Burlingame, CA), as described previously [26]. Double staining of F4/80 and Arg1 has been described previously [26] using monoclonal rat anti-F4/80 (1:75; Cat #: MCA497R; AbD Serotec, Raleigh, NC) and goat anti-Arg1 (1:200; Cat #: sc-18354; Santa Cruz Biotechnology, Inc., Santa Cruz, CA). As described previously [26], estrogen receptor was detected with mouse anti-ERα (1:10; Cat #: NCL-ER-6 F11; Novocastra Laboratories Ltd, Novocastra Laboratories, Ltd, Newcastle upon Tyne, UK) and progesterone receptor was detected with rabbit anti-PR (1:200; Cat #: A0092; DAKO). Images were captured with a Nikon Eclipse TE2000-U fluorescence microscope using a 40x objective. At least 1000 cells and at least 3 sections per animal were analyzed. For CD31 analysis, the images were overlaid with grids containing 240 squares (324 μm^2/square). Blood vessel density is expressed as the percentage of CD31-positive squares. Macrophage density was expressed as number of macrophages per tumor image. Tumors were considered to be ERα positive (ER+) if 10% or more of the total cells counted were ER+ [50]. Mammary tissue sections stained for macrophages, cellular proliferation, and blood vessel density were analyzed by mammary gland epithelial structure: small ducts, large ducts, TEBs, or hyperplastic foci as previously described [26].

Microarray

Total RNA was isolated from mouse tumors using TRIzol reagent (Invitrogen, Carlsbad, CA) and purified using the RT2 qPCR-Grade RNA isolation kit (SABiosciences, Frederick, MD, USA). Agilent Technologies (Santa Clara, CA) 4X44K whole mouse genome microarrays were performed according to manufacturer protocol with linear amplification and 2-color hybridization using total RNA isolated from mouse mammary tumors (Table 2.2). The reference channel was Universal Mouse Reference (as described in [51]) and was labeled with Cy5. Spots that had intensity greater than 10 dpi in at least 80% of samples were selected for subsequent analysis. Data were Lowess normalized and missing data were imputed using k-nearest neighbors with k=10. A total of 10 microarrays were analyzed. Two class Significance Analysis of Microarrays was performed to identify differentially expressed genes between early vs. late tumor onset and high fat diet vs. low fat diet. All statistical analyses were conducted in R using the LIMMA package in Bioconductor. For genes significantly associated ($p<0.05$) with early vs. late tumor onset, gene ontology analyses were conducted using Ingenuity Pathway Analysis.

Metabolic parameters

In the tumorigenesis studies, mice were fasted for 4 hours prior to blood collection and sacrifice. In the pubertal time course studies, plasma were collected from mice fed *ad libitum* to avoid the stress from fasting [52]. Plasma glucose and insulin levels were sampled via cardiac puncture and anticoagulated with ethylenediaminetetraacetic acid (EDTA). Plasma glucose levels were determined by

OneTouch UltraMini (Lifescan, Milpitas, CA) and the insulin levels were determined with the rat/mouse insulin ELISA kit (Millipore, Billerica, MA), according to the manufacturer's instructions.

Statistical analysis

Results are shown as mean ± standard deviation (SD) for body weight, and mean ± standard error of the mean (SEM) for immunohistochemistry analyses. Differences were considered significant at $p < 0.05$ using Student's t-test. Mammary tumor free and overall survival were determined from Kaplan-Meier plots by log-rank tests. Tumor incidence was analyzed by the Chi-square test.

Results

Tumor development and characteristics

After a follow-up of 52 weeks, only 2 mice (4%, n=50) on LFD developed mammary tumors, while 11 mice on HFD (15.7%, n=70) developed mammary tumors (Figure 2.1a). One mouse on HFD developed two tumors in different mammary glands. The majority of the tumors were estrogen receptor negative (ER-) and progesterone receptor negative (PR-) (2/2 in LFD tumors, and 11/12 in HFD tumors). Of the two tumors that developed in LFD-fed mice, one was adenosquamous and the other was glandular. Half of HFD tumors were of epithelial histopathology (6/12; glandular, papillary, cribriform, solid), the remainder tumors were adenosquamous (4/12) and spindle cell (2/12). The mean latency of HFD tumors was 25.9 ± 2.4 weeks post first DMBA treatment and a mean of 35 weeks for

the 2 LFD tumors. Additionally, there was a subset of HFD tumors that developed before tumors developed in LFD-fed mice at 28 weeks of age. This early subset had a predominance of adenosquamous tumors (4/6). The early tumors had a significantly reduced latency compared to late developing HFD and LFD tumors (HFD-early = 20.9± 1.1 vs. HFD late = 33 ± 3.7 weeks of age, p=0.004). HFD also promoted the development of tumors in other organ systems, producing skin tumors, liver tumors and lymphomas, and resulted in significantly worse overall survival (Figure 2.1b).

Our previous work in DMBA-treated BALB/c mice demonstrated significant differential gene expression between early developing and late developing tumors on HFD [26]. Thus, microarray analysis was performed to compare early developing tumors on HFD prior to tumor formation on LFD, and late developing tumors. We identified six genes that were significantly down-regulated in the early tumors: *Smad2*, *Olfr10*, *Gpr75*, *Phc1*, *IFNa2*, and *Gm11937* (data not shown). The canonical pathway and molecular function analyses did not find any significant differences between the early and late tumors (data not shown).

We had previously observed that HFD promoted tumor development in obesity resistant BALB/c mice through increased proliferation, angiogenesis and M2 macrophage recruitment [26]. To determine the basis for HFD promotion of tumorigenesis herein, tumors were also analyzed for tumor cell proliferation, angiogenesis and macrophage recruitment. Tumors that developed in FVB mice on LFD had similar levels of proliferation and angiogenesis to those on HFD (HFD = 7.9

± 0.9%, LFD =9.2 ±1.9%) and angiogenesis (HFD= 16.1 ± 0.02%, LFD= 19.1 ± 0.05% CD31 positive grids) and similar levels of total macrophages (HFD= 20.6 ± 3.6, LFD 18.7) (Figure 2.2a). However, there was a trend toward increased numbers of M2-type macrophages in both the periphery and center of the tumors that developed on HFD (n is too small in LFD group for statistical analysis), suggesting M2 macrophages may contribute to the HFD-associated tumor promotion (Figure 2.2b).

HFD promotes pubertal ductal development and epithelial cell proliferation

Having established that HFD promotes carcinogen-induced tumor development, we sought to examine early effects on mammary gland development near the time when diet was initiated at 3 weeks of age. After only 1 week on diet, at 4 weeks of age, HFD increased the number of terminal end buds (TEBs), the highly proliferative structures found at the tips of the invading ducts during puberty (Figure 2.3a). Shortly after the increase in the number of TEBs, after 2 weeks on diet (5 weeks of age), mice fed a HFD had enhanced ductal elongation (Figure 2.3b-d). By 3 weeks on diet (6 weeks of age), ductal growth in mice on LFD caught up with the accelerated growth in mice on HFD, and both ductal elongation and number of TEBs were similar (Figure 2.3b). By 4 weeks on diet (7 weeks of age), distal ductal elongation reached the limit of the inguinal fat pad and TEBs were reduced and similar in number in mice on both LFD and HFD.

The accelerated ductal development can be partly explained by increased proliferation in the mammary epithelium. Consistent with the pattern of enhanced ductal elongation, ductal proliferation was significantly increased in HFD-fed mice at

the height of pubertal growth after 2 weeks on diet (Figure 2.4); the proliferative effects of HFD were diminished by the end of pubertal growth after 4 weeks on diet (Data not shown). Macrophages participate in the remodeling of the mammary gland during pubertal development [53]. We identified M2-type macrophages by coexpression of F4/80 and Arg1. The majority of macrophages were alternatively activated M2 type (data not shown). There was no difference in the number of macrophages recruited to mammary peri-epithelium or proportion of M1 vs M2 types in mice on LFD or HFD at 2 weeks on diet (data not shown). The accelerated mammary gland development was not a result of early onset of puberty: there was no significant difference in the mean-age of vaginal opening in LFD or HFD-fed mice (29.3 ± 1.8 days and 29.6 ± 2.3 days, respectively).

Analysis of dietary effects on carcinogen-treated mammary glands prior to tumor development

To assess the effects of HFD on tumor progression, we examined DMBA-treated mammary glands at 10 weeks and 16 weeks on diet, prior to the development of palpable tumors. There was a trend toward increased percentage of mice with hyperplastic lesions and but no difference in the mean numbers of lesions per mouse at 10 or 16 weeks on diet in HFD- and LFD- fed mice (Fig 2.5).

Analysis by immunohistochemistry at 10 weeks on diet found increased proliferation in the hyperplastic lesions on either LFD or HFD with a trend to greater proliferation on HFD ($p=0.08$) (Data not shown). There was no difference in proliferation in various mammary gland structures and hyperplasia at 16 weeks on

diet (data not shown). There was also no significant difference blood vessel density by diet at either 10 or 16 weeks on diet (data not shown).

Tumor associated macrophages can play several, sometimes opposing roles in tumor development. Alternatively activated (M2-type) and can exert trophic effects and provide tumor-promoting microenvironment [54]. We identified M2-type macrophages by coexpression of F4/80 and Arg1. Increased total number of macrophages, (M1 and M2), was recruited to peri-epithelial area of the hyperplastic lesions at both 10- and 16- weeks on diet (Figure 2.6). There was also a difference in the proportion of M2 macrophages recruited to hyperplasias between 10 and 16 weeks on diet with M2 macrophages significantly increased ($p=0.01$) at 16 weeks on diet (Figure 2.6).

Effects of diet on weight and metabolic parameters

The change in weight over the entire experimental period is shown in Figure 2.7a. Peripubertal HFD produced a significant increase in body weight only after 1.4 weeks on diet (31 days of age) (Figure 2.7b). Notably, this occurred after the increase in number of TEBs at 1 week on diet.

After the pubertal increase in body weight between 1.4-5 weeks on HFD diet (i.e., 4.4-8 weeks of age), a significant weight loss was observed after the DMBA treatments. Mice on both LFD and HFD regained weight, but HFD-fed mice did not exhibit significant increase in body weight compared with LFD until 14 weeks on diet (17 weeks of age) (Figure 2.7a). HFD-fed mice reached a 24% increase in body

weight at 40 weeks. Thus the HFD-fed mice only reached an obese state near the end of the experiment, whereas the majority of tumors developed prior to 35 weeks.

To determine the effects of diet in metabolic state fasting plasma glucose and insulin levels were obtained at 10 and 16 weeks on diet. No effects of HFD on glucose or insulin levels were observed at 10 weeks on diet. HFD increased fasting glucose after 16 weeks on diet but did not alter fasting plasma (Figure 2.8).

Discussion

HFD promotion of tumorigenesis

HFD initiated in the peripubertal life stage in FVB mice significantly increased tumorigenesis herein compared with a LFD. The interaction of HFD diet and body weight revealed a complex picture with elements of tumor development that appear to be independent of an obesity level weight gain. The regimen of 4 weekly doses of 1mg DMBA described here produced a tumor incidence of 15.7% and 4% in HFD-fed vs. LFD-fed mice, respectively and clearly demonstrated the tumor promotional effects of HFD. However, the low number of tumors developing on LFD (n=2) precluded an extensive comparative analysis of LFD vs HFD tumor types. Thus, our tumor analysis focused on HFD tumors.

DMBA carcinogenesis is known to produce different tumor phenotypes including ER+PR+ tumors [55]. The majority of the FVB tumors on HFD in the present study were ER-PR-. There was a subgroup of early HFD tumors that were ER-PR- and adenosquamous histopathology. These adenosquamous mammary

tumors are similar to early tumors that developed in DMBA-treated HFD-fed obesity-resistant BALB/c mice [26]. Adenosquamous mammary carcinomas are similar to a subtype of human basal-like breast cancer [56]. The findings that HFD promotes the development of these tumors in in FVB mice that gain significant weight and in BALB/c mice that maintain a normal body weight [26] suggest that the HFD promotional effect may be independent of the promotional effect of HFD on weight gain.

We have previously shown that HFD promoted tumor development in normal weight, obesity-resistant BALB/c mice through increased normal epithelial cell, mammary hyperplasia and tumor cell proliferation, increased angiogenesis and pro-tumorigenic M2 macrophage recruitment [26]. The small sample size of LFD tumors makes comparison versus HFD tumors speculative. Interestingly, we found no differences in tumor cell proliferation or angiogenesis in LFD vs. HFD tumors. However, there appeared to be a consistent trend of HFD-associated increase in intra-tumor M2 macrophage infiltration herein, that was also found in HFD-fed BALB/c DMBA-induced mammary tumors [26]. Increased macrophage recruitment was also seen in the BALB/c 4T1 tumor transplant model with HFD started at 4 weeks of age, and HFD also increased tumor burden and metastasis [28]. The relationship between HFD and increased tumor associated macrophages warrants further investigation for understanding the mechanistic basis for HFD promotion of tumorigenesis, and development of therapeutic strategies for the reduction of breast cancer risk and breast cancer treatment.

Microarray analysis revealed six genes that were down-regulated in early HFD tumors. Notably, decreased expression of *Smad2*, *Gpr75*, *Phc1* and *IFNa2* were all associated with poor breast cancer prognosis [57]. Smad2 is a major effector for TGFβ signaling. TGFβ can produce an antiproliferative response by arresting cells in the G_1 phase of the cell cycle [58]. In this pathway, ligand-activated TGFβ receptor complex phosphorylates Smad2, which translocates into the nucleus, associates with Smad4 to form transcriptional complexes with other factors [59]. Important proliferation regulators, including cyclin D1, Cdk4, p21, p27, p15, c-Myc, Rb, p130 and p107 are regulated by the TGFβ/Smad pathway [60]. Oncogenic ras have been reported to negatively regulate Smad2 and inhibit TGFβ signaling [61]. Inactivating mutations, and loss of expression of Smad2 has been reported in human cancer [62]. Knockdown of Smad2 in human breast cancer MDA-MB-231 cells produces a more aggressive phenotype [63]. Downregulation of *Smad2* in early HFD tumors suggest a role of TGFβ signaling in HFD-enhanced tumorigenesis.

Phc1 is part of the chromotin-modifying complex, Polycomb Repressive Complex 1 (PRC1), which is involved in the self-renewal in cancer stem cells [64]. Phc1 deficiency is implicated in initiation of DNA replication in S phase [65]. Loss of heterozygosity in Phc1 has also been implicated in acute lymphoblastic leukemia [66]. With increased number of adenosquamous tumors developing early in HFD-fed mice, it is conceivable that HFD caused epigenetic modifications that altered the mammary progenitor cell differentiations.

IFNa2 is a type I interferon and is a protypical antitumor cytokine, regulating the immune system with antiangiogenic and proapoptotic effects [67]. IFNa-2a and IFNa-2b are FDA-approved therapeutic proteins for hepatitis C, and has been used with some success for treatment of several types of hematologic malignancies, melanoma, renal carcinoma and Karposi sarcoma [68]. Macrophages activated by IFN alpha lose their proliferative capacity and gain phagocytic activities [69]. Consistent with down-regulation of *IFNa2* in early HFD tumors, we observed a trend of increased number of macrophages in hyperplastic lesions after 10 and 16 weeks on HFD. IFNa is a major regulator for T cells and NK cells [70], and it is suggestive that T cells, NK cells, and their cytotoxic activity maybe reduced by HFD.

HFD effects on normal pubertal mammary gland development

Mouse strains vary significantly in their response to HFD with regard to pubertal mammary gland development [24]. HFD-fed FVB mice herein exhibited accelerated pubertal mammary gland development. This in contrast to the inhibition of pubertal mammary gland development observed in HFD-fed, obesity-prone C57BL/6 mice [24]. In FVB mice the HFD-enhanced initiation of TEB development preceded an increase in body weight. Thus, initial HFD- induced weight gain in FVB mice appeared to be uncoupled from the initial proliferative effects of HFD on mammary glands. Increased pubertal mammary gland development was also reported in HFD-fed, normal weight obesity-resistant BALB/c mice [24], further suggesting that the some of the proliferative effects of HFD involve pathways independent of weight gain.

Ductal elongation in puberty is predominantly driven by estrogen [71]. Although estrogen levels were not directly measured in the present experiment, vaginal opening is driven by estrogen and can serve as a surrogate for estrogen activity. In this regard, there was no difference in age at vaginal opening between HFD- and LFD-fed mice. Previously, we found that estrogen levels were not altered in either obesity-resistant BALB/c mice or obesity-prone C57Bl/6 mice on HFD [24].

Pre-tumor effects of HFD in DMBA-treated mammary glands

DMBA-induced mammary tumors are preceded in time by the development of hyperplastic lesions. There was a trend to increased numbers of mammary glands with lesions and numbers of lesions in HFD mammary glands at 10 weeks on diet (13 weeks of age and 8 weeks post 1st DMBA treatment). At this time point there was no difference in weight between HFD- and LFD-fed mice. Analysis of HFD and LFD mammary glands for proliferation in mammary epithelial cells and hyperplastic lesions showed a trend to increased proliferation in hyperplastic lesions at 10 weeks on diet, also at a time when there was no difference in body weights, There was no difference in proliferation in various mammary structures or hyperplastic lesions at 16 weeks on diet. Furthermore, there were no differences in blood vessel density at either 10 or 16 weeks on diet. These results contrast with the significant HFD increase in proliferation and angiogenesis in BALB/c at 10 weeks on diet [26]. This suggests that in FVB mice HFD promotional effects were most significant with regard to HFD-associated increase in macrophage recruitment.

Tumor associated macrophages can play several, sometimes opposing roles in tumor development. The Arg1- macrophages indicate more classically activated M1-type, which could perform anti-tumor role [54]. Macrophages in response to CSF-1, or NF-kB are alternatively activated (M2-type) and can exert trophic effects and provide tumor-promoting microenvironment [54]. At 10 weeks on diet, compared to normal structures, the HFD hyperplastic lesions were associated with an increased number of Arg- and Arg+ macrophages with Arg- M1 macrophages predominating. By 16 weeks on diet there were fewer M1 macrophages and a greater proportion of M2 macrophages associated with HFD lesions that may have contributed to the overall promotional effect of HFD. Previously, we found that HFD increased the number of DMBA-induced lesions in BALB/c mice at 10 weeks. The increase was more modest at 16 weeks. In both strains, there were increased numbers of macrophage polarization toward the M2-type in HFD lesions, which could have facilitated their tumor progression. Our finding of increased macrophage presence is consistent with reports that HFD up-regulated genes in pathways associated with inflammation [72, 73].

Relationship between HFD and weight gain on tumor promotion

The effect of HFD on body weight produced a complex pattern in the current experiments in the FVB strain. Diets were initiated at 3 weeks of age and the first significant HFD-induced increase in body weight was noted at 4.4 weeks (31 days of age) of age. This weight gain occurred after the initial HFD-associated development of TEBs and proliferative changes in the normal peripubertal mammary gland at 4

weeks of age (28 days of age). By 7 weeks of age HFD-fed mice weight 14% more than LFD-fed mice; this weight gain did not constitute and obese state. Significant weight gain continued during DMBA treatment 5-8 weeks of age. During this period the greater number of lesions in HFD-fed mice, may have resulted from an increased number of DNA damage events. The bioavailability of lipophilic carcinogen DMBA and its activated metabolites may be enhanced when HFD-fed mice had increased body weight during administration of carcinogen. HFD has been reported to increase AhR, which is a receptor for DMBA and its metabolites [74], and thus increase DMBA carcinogenicity. Between 9 and 17 weeks of age the mice on HFD and LFD both lost weight at first and then re-gained weight with no difference in body until 17 weeks of age. It is difficult access the effects of HFD at 13 and 19 weeks of age when pre-tumor analyses were carried out, since this was a period of no or minimal weight gain. The 4 early adenosquamous HFD tumors arose at 19-24 weeks of age at a time where there were only small weight gains, suggesting the HFD effect was not producing an obese weight range. Finally, weight gain continued in HFD-fed mice to the termination of the experiment, at which time the maximum weight gain was 24% above LFD weight and was in the obese range. Most of the HFD tumors arose before this weight gain was reached. Taken together. These results suggest either that the HFD promotional effect occurred in a normal weight range or that this range of weight gain was sufficient to be promotional. Additional insight can be obtained from the effect of HFD on metabolic parameters of glucose and insulin levels. From 10 to 16 weeks on diet there were no indications from plasma glucose or insulin levels that HFD produced significant metabolic changes.

This suggests that the effects of HFD in the FVB strain were tumor promotional without a significant metabolic effect.

Summary and Conclusions

Taken together, the present results in the FVB mouse strain indicate that the promotional effects of HFD initiated at peripuberty on carcinogen-induced mammary cancer was largely independent of weight gain, particularly in the obese weight range. Furthermore, HFD promoted a subset of early adenosquamous tumors which was also observed in HFD-fed normal weight BALB/c mice suggesting that early age exposure to HFD may be promotional for a specific tumor subtype. Epidemiological data is lacking for the association of HFD consumption in young premenopausal women and breast cancer subtypes [19]. Other studies have reported positive associations between HFD and receptor positive disease but not receptor negative disease [16]. However, a number of confounding variables such the numbers of pre vs postmenopausal women analyzed and the age at HFD dietary intake that could preclude an accurate assessment of early life HFD and breast cancer subtype. In this regard we have found a significant association of young age but not with older adult age consumption of HFD and increased early development of ER-PR- tumors in normal weight BALB/c mice[26].

Contributing factors to increased incidence of mammary cancers such as increased proliferation and angiogenesis differed between HFD-fed FVB and BALB/c mice. However notably, HFD-associated increase in pro-tumorigenic (M2) macrophage recruitment was a common factor in both strains. Thus, we speculate

that a similar effect of HFD on immune function may provide clues to the basis for the epidemiology findings of increased breast cancer risk in young premenopausal, normal weight women who consume a diet high in saturated animal fat.

CHAPTER 3

Pubertal and Adult Windows of Susceptibility to High Fat Diet in *Trp53*-null Mammary Tumorigenesis

Introduction

The incidence of breast cancer has remained stable despite recent advances in detection, treatment options and survival [2]. Effective prevention strategies are needed to combat breast cancer. Lifestyle modifications, especially changes in diet are heavily investigated as potential preventative measures [15]. Some studies reported that a western diet, rich in saturated fat, is associated with increased breast cancer risk [75]. However, meta-analyses examining the association of total fat and saturated fat intake with breast cancer risk are inconsistent, partly because of differences in study design, dietary classification, and varied baseline breast cancer incidence among the diverse populations studied [76-80]. The interaction of fat intake with breast cancer risk may also be subtype specific [16]. While high fat diet (HFD) often leads to obesity, a recent analysis of the Nurses' Health Study II identified adolescent and early adulthood intake of high animal fat to increase breast cancer risk only in normal weight women, suggesting dietary effects in tumor promotion may be obesity independent [19].

Human and rodent models have demonstrated that the mammary gland is sensitive to environmental and dietary influences during puberty [81, 82]. We previously reported that HFD initiated in puberty significantly reduced the latency of 7, 12-dimethylbenz[a]anthracene (DMBA)-induced tumors in the absence of

obesity [26] and that a HFD restricted to puberty similarly reduced the latency of DMBA-induced tumors [29]. Mice overexpressing *HER2/neu* had increased development of second tumors when HFD was introduced in pubertal mice at 4 weeks of age [27], but tumor incidence was not affected when HFD was introduced to adult mice at 10 weeks of age [30], again suggesting the importance of timing in HFD exposure. In this regard, the human epidemiological study by Linos *et al.* [83] specifically indicates adolescent exposure to total dietary fat as a risk factor for premenopausal breast cancer.

DMBA needs to be introduced in mice during puberty to efficiently initiate mammary tumors [55]. To circumvent the potential confounding interaction of pubertal HFD with DMBA exposure, the present study investigated the effects of pubertal versus adult exposure to HFD on mammary tumorigenesis in obesity resistant BALB/c mice, using the *Trp53-null* transplantation model. *Trp53* is one the most frequently mutated genes in human breast cancer [34]. We found both pubertal and adult windows of susceptibility to HFD. Tumor cell proliferation, angiogenesis, and inflammatory processes were all significantly altered by HFD exposure at any life stage. Adult HFD exposure uniquely increased the occurrence of estrogen and progesterone receptor negative (ER- PR-), poorly differentiated spindle cell carcinomas. These findings further implicate HFD as a risk factor in the occurrence of mammary cancer.

Material and Methods

Mice

BALB/c *Trp53*$^{+/-}$ breeding mice were obtained from Dr. D. Joseph Jerry (University of Massachusetts, Amherst MA), and *Trp53-null* mice were generated as described [35]. The *Trp53-null* tissue donor mice were maintained on chow diet before mammary gland collection at eight weeks of age. Wild-type recipient female BALB/c mice were purchased from Charles River (Portage, MI) at 3 weeks of age. Mice were randomly assigned into four diet groups (see Diets). Food and water were provided *ad libitum*. Animals were housed in a standard laboratory housing environment with a 12:12 h light–dark cycle, at 20 to 24°C with 40 to 50% relative humidity. All animal experimentation was conducted in accord with accepted standards of humane animal care under guidelines approved by the All University Committee on Animal Use and Care at Michigan State University.

Trp53-null model

Fragments of donor mammary epithelium were collected from female BALB/c *Trp53-null* mice at 8 weeks of age, and transplanted into the cleared inguinal mammary fat pads of 3-week-old female wild type mice as previously described [84, 85]. To minimize donor bias from secondary genetic alterations, mammary duct fragments from 4 donor mice were transplanted to recipient mice in each diet group in equal distribution. Body weights and food consumption were monitored weekly. Animals were palpated for tumor development twice a week

starting at 13 weeks of age. Tumors were harvested at 1 cm in diameter. Portions of tumors and mammary glands were formalin-fixed, paraffin embedded for H&E and immunohistochemistry, and the remaining portions of tumors were snap-frozen for later RNA isolation. Mice were monitored for 500 days, and at termination of the studies, mammary glands were formalin-fixed and processed as whole mounts to evaluate transplantation success rate. Transplantation success rates were 59%, 77%, 64% and 72% for the LFD, HFD, LFD-HFD, HFD-LFD groups, respectively. Mammary glands that had no epithelium present were excluded from the survival analysis.

Diets

Control low fat diet (D11012202; 10% kcal fat) (LFD) and high fat diet (D11012204; 60% kcal fat) (HFD) were purchased from Research Diets (New Brunswick, NJ). The majority of the kcal fat in HFD derives from lard (54.5% kcal), while the remaining 5.5% kcal fat derives from corn oil. LFD contained 4.5% kcal fat from lard and 5.5% kcal fat from corn oil. See Table 2.1 for detailed composition of the diets. For the continuous LFD and HFD groups, diets were initiated after transplantation at 3 weeks of age and maintained throughout the studies. For the HFD-LFD and LFD-HFD groups, mice were initially fed one diet from 3 weeks until 10 weeks of age, and then switched to the other diet thereafter (Figure 3.1).

Immunohistochemistry

5μm tumor sections were deparaffinized and rehydrated, as previously described [26]. Antigen retrieval was accomplished by autoclaving at 121°C and 15 psi for 30 minutes in citrate buffer (pH 6.0). For blood vessel density determinations, CD31 was detected with rabbit polyclonal anti-CD31 (1:50 in PBS–0.5% Triton X-100; Cat #: AP15436PU-N; Acris Antibodies, Inc., San Diego, CA) at RT for 2 hours. Images were captured using a Nikon Eclipse E400 light microscope (Nikon, Inc., Melville, NY) with a 40X objective lens. The images were overlaid with grids containing 240 squares (324 μm^2/square). Blood vessel density is expressed as the percentage of CD31-positive squares. For proliferation, PCNA was detected using goat polyclonal anti-PCNA (1:100 in PBS–0.5% Triton X-100; Cat #: sc-9857; Santa Cruz, Biotechnology, Inc., Santa Cruz, CA) at 4 ^{O}C overnight. For macrophage detection, double staining of F4/80 and Arg1 has been described previously [26] using monoclonal rat anti-F4/80 (1:75 in PBS–0.5% Triton X-100; Cat #: MCA497R; AbD Serotec, Raleigh, NC) and goat anti-Arg1 (1:200 in PBS–0.5% Triton X-100; Cat #: sc-18354; Santa Cruz Biotechnology, Inc.). As described previously [26], estrogen receptor was detected with mouse anti-ERα (Novocastra Laboratories Ltd, NCL-ER-6 F11, 1:10) and progesterone receptor was detected with rabbit anti-PR (DAKO, A0092, 1:200). Tumors were considered to be ERα positive (ER+) if 10% or more of the total cells counted were ER+ [50]. Cytokeratin-5 (K5) and cytokeratin-18 (K18) staining has been previously [86, 87] described using (Covance, PRB-160P, 1:500) and mouse monoclonal antibody (Abcam, ab668-100, 1:75). Immunofluorescent staining was completed with appropriate secondary antibodies. All

immunofluorescence sections were counterstained with 4', 6-diamidino-2-phenylindole (DAPI) to visualize nuclei. Images were captured with a Nikon Eclipse TE2000-U fluorescence microscope (Nikon, Inc.) using a 40x objective. At least 1000 cells and at least 3 sections per animal were analyzed. For proliferation, cells were scored positive with the presence of speckled nuclear localization of PCNA [88]. Macrophage density was expressed as the number of F4/80 positive cells per tumor image.

TUNEL

5μm tumor sections were deparaffinized and rehydrated. Terminal deoxynucleotidyl transferase dUTP nick end labeling (TUNEL) analysis was performed using the TdT-FragEL DNA Fragmentation Detection Kit (EMD Millipore, Billerica, MA) following the manufacturer's directions. At least 1000 cells and at least 3 sections per animal were analyzed.

Metabolic parameters

Plasma glucose and insulin levels were measured from samples collected at sacrifice from non-fasting tumor-bearing animals, as previously described [26]. Plasma glucose levels were determined by OneTouch UltraMini (LifeScan, Inc., Milpitas, CA) and the insulin levels were determined with the rat/mouse insulin ELISA kit (EMD Millipore), according to the manufacturer's instructions.

Microarray analysis

Agilent Technologies (Santa Clara, CA) 4X44K whole mouse genome microarrays were performed according to manufacturer protocol with linear amplification and 2-color hybridization using total RNA isolated from mouse mammary tumors (Table 3.1). The reference channel was Universal Mouse Reference (as described in [51]) and was labeled with Cy5. Spots that had intensity greater than 10 dpi in at least 80% of samples were selected for subsequent analysis. Data were Lowess normalized and missing data were imputed using k-nearest neighbors with k=10. A total of 32 microarrays were analyzed. Two class Significance Analysis of Microarrays was performed to identify differentially expressed genes between early vs. late tumor onset among all tumors and among spindle cell and epithelial cell carcinomas separately, pubertal HFD vs. LFD, and spindle cell vs. epithelial carcinoma. All statistical analyses were conducted in R using the LIMMA package in Bioconductor. For genes significantly associated ($p<0.05$) with early vs. late tumor onset, gene ontology analyses were conducted using Ingenuity Pathway Analysis. The data discussed in this publication have been deposited in the National Center for Biotechnology Information Gene Expression Omnibus (GEO) [89] database and are accessible at accession number [GEO: GSE74294] [Puberty-specific promotion of mammary tumorigenesis by a high animal fat diet in P53 -/- mice http://www.ncbi.nlm.nih.gov/geo/query/acc.cgi?acc=GSE74294 Access date: 24 Oct 2015].

Statistical analysis

Results are shown as mean ± standard deviation (SD) for body weight, and mean ± standard error of the mean (SEM) for immunohistochemistry analyses. Differences were considered significant at $p < 0.05$ using Student's t-test or analysis of variance (ANOVA) followed by the Tukey multiple comparison test, as appropriate. Mammary tumor free survivals were determined from Kaplan-Meier plots by log-rank tests. Tumor incidence was analyzed by the Chi-square test.

Results

Either peripubertal or adult exposure to HFD promotes tumorigenesis

Kaplan-Meier analysis revealed that the one-year mammary tumor incidence in mice receiving *Trp53-null* mammary transplants (Figure 3.2a) was significantly increased by peripubertally-restricted HFD (HFD-LFD, 39%; 2.2-fold; p=0.042), as well as by HFD restricted to adulthood (LFD-HFD, 47%; 2.6-fold; p=0.009) compared to LFD (17%). Continuous HFD also caused a 1.7-fold increase in tumor incidence by one year of age (HFD 31%; p = 0.16), but the difference did not reach statistical significance. Further follow up of tumor development up to 500 days of age at the end of the study (Figure 3.2b) showed tumor incidence was increased by continuous HFD (HFD, 81%; 1.8-fold; p=0.046) and adult HFD (LFD-HFD, 89%; 2-fold; p=0.006) compared to control LFD (54%); the tumor promotional effects of early HFD (HFD-LFD, 70%; 1.6-fold; p=0.13) were less dramatic when viewed over the longer time course and also showed a trend toward increased tumor incidence.

There were no significant differences in tumor latency by diet treatments (data not shown).

Tumor characteristics

Tumors of multiple histopathologic types (Figure 3.3) developed in *Trp53-null* mammary transplants. Regardless of the diet treatment, the majority of tumors contained an epithelial component. However, some of the tumors were poorly differentiated spindle cell carcinomas. LFD-HFD mice had a significantly increased number of spindle cell carcinomas per transplant compared to mice on other dietary regimens ($p=0.02$) (Figure 3.3a). The majority of the epithelial tumors (63-82% among the dietary regimens) were ER- PR- and did not vary significantly by histological types or diet treatment and all spindle cell tumors were ER- PR- (Table 3.2).

Since uncontrolled proliferation and escape from apoptosis are hallmarks of cancer [90], we measured tumor cell proliferation and apoptosis by quantifying nuclear localization of PCNA and TUNEL, respectively. Continuous HFD, HFD-LFD, and LFD-HFD all significantly increased tumor cell proliferation by 1.8 to 1.9 fold ($p<0.01$) compared to tumors from LFD mice (Figure 3.4a). To see if this effect was specific to tumor cells, we also measured the effect of diet on proliferation in normal tissue. No significant effects on proliferation were observed in normal tissue of 19-week old mice, prior to the appearance of any tumors (data not shown). Within each diet group, no difference in tumor cell proliferation was found between the epithelial and spindle cell tumors (data not shown). In contrast to tumor cell

proliferation being enhanced by HFD at either puberty or adulthood, apoptosis was significantly decreased ($p<0.05$) only in tumors from mice fed LFD-HFD (0.58 fold of that in LFD) and continuous HFD (0.59 fold of that in LFD) (Figure 3.4b).

Because HFD was associated with increased angiogenesis in DMBA-induced tumors, we analyzed intratumoral vascularization (Figure 3.5). Epithelial tumors occurring in mice exposed to HFD at either puberty or adulthood showed 1.7 to 1.8 fold increased vascularization compared to mice fed LFD. Both HFD-LFD and LFD-HFD were sufficient to increase blood vessel density similarly to continuous HFD. Diet had no significant effect on spindle cell tumors, but independent of diet, spindle cell tumors had higher blood vessel density compared to epithelial tumors ($p=0.02$). No significant effects on vascularity were observed in normal tissue of 19-week old mice, prior to the appearance of any tumors (data not shown).

Macrophages play important roles in normal mammary development and tumorigenesis [91]. We examined both intratumor macrophage localization and the extent of M2 (i.e., Arg1+) polarization in these macrophages (Figure 3.6). Increased numbers of macrophages were observed under all diet regimens that included a period of HFD exposure compared to continuous LFD ($p<0.05$). The majority of macrophages were Arg1- (i.e., likely M1, classically activated) in all tumors across all diet treatments. However, HFD, HFD-LFD and LFD-HFD tumors all additionally exhibited significantly increased numbers of M2 macrophages compared to LFD tumors ($p<0.05$). The enhanced recruitment of macrophages was independent of

tumor histopathology and independent of the time of tumor occurrence (data not shown).

Microarray analysis of gene expression in tumors

We thought it would be productive to examine early versus later occurring tumors using a time threshold distinguishing between the time period where mice fed HFD-LFD showed significantly higher tumor incidence and the longer time period where significance was not observed (see Figure 2). Gene ontology analyses of microarray data comparing early occurring tumors (i.e., latencies 48 weeks and less) to later occurring tumors identified a number of molecular functions as being upregulated in early occurring tumors (Table 3.3). The two most statistically significant were "Immunological Disease: systemic autoimmune syndrome" (p=5.19E-14) and "Endocrine System Disorders, Gastrointestinal Disease, Immunological Disease, Metabolic Disease: insulin-dependent diabetes mellitus" (p=5.19E-14). A similar analysis of early versus late-occurring tumors that considered the spindle cell tumors separately from the other epithelial tumors found no significant differences between early and late occurring spindle cell tumors (data not shown), but found the following molecular functions upregulated in the early occurring epithelial tumors to high statistical significance (Table 3.4): "Immunological Disease: systemic autoimmune syndrome" (p=9.18E-13); "Endocrine System Disorders, Gastrointestinal Disease, Metabolic Disease: diabetes mellitus" (p=9.18E-13); "Endocrine System Disorders, Gastrointestinal Disease, Immunological Disease, Metabolic Disease: insulin-dependent diabetes mellitus"

(p=8.51E-14). Comparison of spindle cell tumors to the various epithelial tumors revealed 1594 upregulated and 1840 downregulated significant genes. No significant canonical pathways were identified and, while some significant upregulated molecular functions were identified, none of the molecular functions had levels of significance approaching those identified in the aforementioned analyses (Table 3.5). While microarray analysis comparing mice exposed to HFD during puberty (HFD and HFD-LFD) to those exposed to LFD during puberty (LFD and LFD-HFD) found 55 upregulated genes (GEO: GSE74294), no canonical pathways or molecular functions were identified (data not shown). The tumor samples from the individual dietary regimens did not provide adequate power for a 4-way analysis (data not shown).

Dietary effects on metabolic parameters

BALB/c mice were previously reported to be obesity resistant on HFD [24]. In the present study, we observed modest weight gain in HFD and LFD-HFD mice (Figure 3.7). However, the weight gain was neither correlated with altered non-fasting plasma glucose levels (Figure 3.8a) nor non-fasting plasma insulin levels (Figure 3.8b) in tumor-bearing mice. As the mice aged, there was a trend towards increased plasma glucose levels, but not plasma insulin levels, in all diet groups (data not shown).

Discussion

In *Trp53-null* initiated tumors, we have identified two different life stage periods of increased tumor development in response to HFD. HFD restricted to the peripubertal window (HFD-LFD) was sufficient to increase tumor incidence in mice at one year of age, but the magnitude of this promotional effect diminished over a longer time frame; the effects of pubertal HFD were evident in younger adults. Despite switching to LFD in adulthood, the short 7 weeks of peripubertal HFD exposure promoted tumor cell proliferation, increased angiogenesis, and increased recruitment of total and M2-type macrophages, similarly to lifelong or adulthood-restricted exposure to HFD.

Trp53-null initiated tumors were also promoted by exposure to HFD limited to adulthood. This differs from our findings on HFD exposure in the DMBA model, where pubertal exposure was required for enhanced tumorigenesis [26, 29]. Perhaps, the longer time course of tumorigenesis for the *Trp53-null* tumors simply provides a longer window for adult HFD effects to occur than does the shorter window for adult HFD exposure in the DMBA model. Over a longer 500-day time frame, adulthood-restricted HFD (LFD-HFD) and lifelong HFD initiated in puberty significantly increased tumor incidence. In addition to promoting tumor cell proliferation, HFD and LFD-HFD diets enhanced angiogenesis, increased recruitment of total and M2-type macrophages, and promoted tumor cell survival by reducing apoptosis. HFD and LFD-HFD exposures were also associated with a modest body weight gain of 14-17%. This increase in body weight was within a

normal range and did not reach an obese status. Furthermore, the metabolic effects of LFD-HFD on plasma glucose and insulin were indistinguishable from the LFD control. In addition to increasing overall mammary tumor incidence, only LFD-HFD, among the dietary regimens, significantly increased the incidence of spindle cell carcinoma, which was previously characterized to have many features of epithelial-to-mesenchymal transition (EMT) and a gene expression profile similar to the claudin-low (CL) intrinsic subtype of human breast cancer [92]. About 65-80% of CL human breast cancers are reported to be ER- PR- [93]. With our *Trp53-null* mammary transplant model, all spindle cell carcinomas were ER- PR-. CL tumors typically lack luminal differentiation markers [93]. We confirmed that the majority of the spindle cell tumors lack expression of K5 and K18 (data not shown). Genomic analysis of CL breast cancer identified a high level of genomic instability with many gains and losses [94]. This suggests that CL tumors are likely driven by several oncogenic events. It is noteworthy that both HFD and LFD-HFD mice experience lengthy exposure to HFD, yet the dramatic increase in spindle cell carcinoma is specific to LFD-HFD. Examination of macrophage levels in pre-tumor mammary glands showed that macrophage levels were only elevated in mice exposed to a pubertally restricted HFD (i.e., HFD-LFD; $p=0.061$). Perhaps this increased number of macrophages partially suppresses the occurrence of spindle cell carcinomas under these dietary regimens, while LFD-HFD mice, having fewer macrophages in pre-tumor tissue, are more permissive for their occurrence.

Ingenuity Pathway Analysis based on microarrays of the tumors found that early occurring tumors upregulated molecular functions associated with type 1

diabetes and systemic autoimmune syndrome. The genes identified across these molecular functions are almost completely identical and, while associated with the pathology of diabetes, are genes more generally associated with autoimmune activity. This is likely related to the *Trp53-null* genotype of the mammary epithelia in these studies. A *Trp53* polymorphism that affects its function is associated with susceptibility to several autoimmune disorders, including systemic lupus erythematosus [95-98], Hashimoto's thyroiditis [99], and rheumatoid arthritis [100]. Somatic *Trp53* mutations were identified in the synovia of rheumatoid arthritis patients [101-105]. A likely mechanism for a *Trp53-null* genotype mediating enhanced autoimmune activity is dysregulation of apoptosis. *Trp53* drives *CD200* expression, which reduces immune reactivity to apoptotic self-antigens [106]. Another apoptotic related function of *Trp53* is the induction of the pro-apoptotic death domain 1α protein (DD1α), which is involved in macrophage recognition and clearance of apoptotic cells [107]. DD1α-deficient mice show autoimmunity and inflammation associated with their inability to clear apoptotic cells. The failure to express *CD200* and/or *DD1*α may be the basis for enhanced autoimmunity under *Trp53*-deficiency. Further, it should be noted that that dietary treatments were largely without effect on glucose and insulin levels, highlighting the immune rather than metabolic significance of the identified molecular functions. It is interesting that increased autoimmune activity is identified in early versus later occurring tumors. An age-related decline in T cell activity is well-established in mouse models [108]. At the same time, there is also an increased abundance of immunosuppressive Treg cells with age [109].

We previously reported that a pubertally initiated lifelong HFD decreased DMBA-induced tumor latency, partly by increasing tumor proliferation, angiogenesis and recruitment of M2-type macrophages. Recently, we reported that only peripubertal HFD, but not HFD restricted to adulthood, promoted DMBA-induced tumors [29]. A similar pubertal window of susceptibility was identified in the MMTV-neu model, where only pubertally initiated HFD promoted development of second tumors [27]. However, here we find that HFD confers similar proliferative, angiogenic and inflammatory changes to *Trp53-null* initiated tumors, when given during either puberty or adulthood. This discrepancy in the windows of susceptibility to HFD between tumor models might be caused by differential sensitivity to HFD between tumor subtypes. Indeed, recent human epidemiological studies suggest that this may be the case in humans [16]. In the DMBA carcinogenesis model, a significant proportion of the early developing tumors from mice fed a peripubertal HFD were adenosquamous carcinomas, which are rare in the *Trp53-null* transplant model. In contrast, the spindle cell carcinomas promoted by HFD restricted to adulthood in the *Trp53-null* transplant model are rare in other murine carcinogenesis models [92].

A limited number of randomized, controlled studies of dietary intervention to prevent breast cancer have been carried out with mixed conclusions. One study that focused on women with high mammographic density found no reduction in breast cancer risk with reduced dietary fat [110]. Another study focusing on post-menopausal women, while finding no significant protective effect for low fat intervention, reported a trend toward a protective effect in women with highest

baseline fat intake [111]. Here, we found that switching mice from a pubertal HFD to an adult LFD does not confer short-term protective effects. 1 year tumor-free survival was inferior in our HFD-LFD group compared to its continuous LFD control. Pubertal HFD followed by a longer term LFD for more than 1 year failed to show significantly increased risk of mammary tumors over that occurring in mice fed lifelong LFD, but whether this reflects a reduction in the risk posed by pubertal HFD or alleviation of adult-specific dietary risk is unclear because HFD restricted to adulthood poses a significant risk in itself. Nonetheless, the existence of both pubertal and adult windows of susceptibility to HFD and the potential alleviation of HFD-associated risk demonstrated in this study offer hope for using dietary intervention as a breast cancer prevention strategy. However, the profound effects of pubertal HFD on tumor development highlight the challenges for successful dietary intervention programs and the need for early life intervention strategies.

Obesity/high body mass index (BMI) (BMI $\geq$ 25 kg/m^2) is a well-established risk factor for post-menopausal breast cancer [20]. However, normal weight women who consume high saturated fat and high animal fat diets may also have increased breast cancer risk regardless of menopausal status [19]. In the current study, modest weight gain of 14-17% was observed in BALB/c mice fed lifelong and adulthood-restricted HFD. The modest weight gain is in line with previous studies in BALB/c mice demonstrating their resistance to HFD-induced obesity [24, 26, 29]. Independent of obesity, both pubertal and adult HFD enhanced tumor cell proliferation. We previously reported upregulation of *Tnfsf11* (receptor activator of nuclear factor κB ligand, RANKL) RNA expression in pubertal BALB/c mice fed HFD

for 4 weeks, as well as elevated levels of plasma IGF-I [26]. DMBA-induced tumors from mice fed lifelong HFD had increased expression of proliferative genes, including *Bmp7*, *Ccdn2*, *Inha*, and *Igf1r* [26]. We also found that early-occurring DMBA-induced tumors from mice fed lifelong and pubertally restricted HFD showed upregulation of canonical pathways associated with proliferative processes (i.e., G_1/S checkpoint regulation, G_2/M DNA damage checkpoint regulation, cyclins and cell cycle regulation, antiproliferative role of TOB in T cell signaling, mTOR signaling, purine nucleotides de novo biosynthesis II, cell cycle control of chromosomal replication, and molecular mechanisms of cancer) [29]. Also in a non-obesogenic context, HFD stimulated growth of injected 4T1 cells in the BALB/c mammary fat pads, and promoted liver and lung metastases [28]. In the latter study, HFD promoted tumors that showed increased proliferation with upregulation of Ki67, CDK2, CDK4, Cyclin D1, Cyclin A, and IGF-I proteins. Collectively, our findings and those of others suggest that a diet rich in saturated fatty acids may promote proliferation in mammary tumors. Our earlier studies found that HFD stimulated proliferation in normal mammary epithelium [24, 26, 29], however we did not observe this in the current study. The proliferative response of normal epithelium to HFD may be a property of the peripubertal window of susceptibility. Alternatively, a proliferative response to HFD in normal epithelium may require intact *Trp53*.

In this study, we found that vascularization and M2 macrophage infiltration of tumors were increased by either pubertal or adult HFD. Increases in the total number of macrophages in normal mammary epithelium of 19-week old mice fed a pubertally restricted HFD approached significance, and this might indicate the

critical role of macrophages in the pubertal window of susceptibility, as well as the sensitivity of the pubertal window to HFD effects. Tumor-associated M2 macrophages are known to promote the growth of tumors through support of angiogenic and tissue remodeling processes, as well as immune suppression [112]. Their presence at early pre-neoplastic stages in tumor development suggests a critical role in tumorigenesis [113]. The association of increased M2 macrophages with increased vascularization in tumors of mice subjected to HFD may be causal. HFD can induce low-grade inflammation after feeding [114]. It has been proposed that this occurs through increased permeability of the gut allowing bacterial endotoxin to enter the circulation and induce inflammation [114, 115]. Saturated fatty acids may also directly modulate inflammatory processes through toll-like receptor 4 (TLR4) [116]. Palmitic acid, the most abundant fatty acid component of lard [117], has been implicated in both TLR2 and TLR4 signaling [118-121].

Summary and Conclusions

In summary, our findings show that exposure to HFD during either puberty or adulthood is sufficient to increase the incidence of *Trp53-null* mammary tumors in the absence of obesity. Pubertally restricted HFD increased tumor incidence in adults prior to 1 year of age. Notably, HFD restricted to adulthood not only increased the incidence of mammary tumors, but specifically increased the incidence of spindle cell carcinomas that resemble claudin-low breast cancer. HFD exerts potent effects regardless of the exposure window. Irrespective of histopathology, tumors that developed in mice fed lifelong HFD, pubertal HFD, and

adult HFD all showed enhanced tumor proliferation, angiogenesis and macrophage recruitment. A HFD restricted to adulthood in the *Trp53-null* transplantation system for mammary tumorigenesis may be a useful animal model for human claudin low breast cancer.

Importantly, the collective results of this study on *Trp53-null* mammary tumorigenesis and with our prior studies on DMBA-induced mammary tumorigenesis [26, 29] demonstrate a peripubertal window of susceptibility to the promotional effects of HFD, indicating the potential of an early life dietary prevention strategy to reduce the risk of breast cancer.

CHAPTER 4

Conclusions

The results presented in this study agree with the majority of published studies in mice showing that a pubertally initiated HFD promoted mammary tumorigenesis. This study indicated that HFD increased tumor incidence in mice either resistant or susceptible to diet-induced obesity. In both mouse strains, HFD were found to increase the number of Arg1+ M2-type macrophages associated with early dysplastic lesions in the DMBA model and mammary tumors in the *Trp53*-null model. Proliferation and angiogenesis, however, were enhanced only in mammary tumors in obesity-resistant BALB/c mice. Puberty has been hypothesized to be a window of susceptibility to environmental factors including diet. The results from this study, however, showed that pubertal exposure to HFD is not required for the tumor promotional effects in the *Trp53*-null model. Both pubertal and adult exposure to HFD altered tumor characteristics and may represent separate windows of susceptibility in that model.

Previously, it was found that HFD decreased latency of DMBA-induced tumors in obesity-resistant BALB/c mice [26]. Evidence presented here from the BALB/c *Trp53*-null model further confirmed that HFD was sufficient to enhance tumorigenesis independent of obesity. These findings are consistent with human epidemiological studies showing that high animal fat and high saturated fat increased breast cancer risk in normal weight women [19]. Epidemiological studies found obesity to be mildly protective against risk of premenopausal breast cancer

[20]. However, in FVB mice, the weight gain obtained on HFD was not sufficient to protect against HFD in increasing tumorigenesis. In normal weight BALB/c mice, tumors from HFD-fed mice had increased proliferation, but HFD gave no proliferative advantages to hyperplastic lesions and tumors in FVB mice that show weight gain. Similarly, tumor angiogenesis was enhanced by HFD in normal weight BALB/c mice, but not in FVB mice. One hypothesis is that weight gain and associated processes counteracted the proliferative effects of HFD in the FVB strain. It remains to be discovered what pathways contributed to the varied proliferative and angiogenic response to HFD in the two mouse strains.

In the non-obesogenic context, systemic IGF-I was elevated in BALB/c mice after 4 weeks on HFD, and *Igf1r* expression was elevated in HFD tumors [26]. Similarly, in models of diet-induced obesity, GH/IGF pathways have also been proposed to mediate the promotional effects of HFD. In adult mammary glands, HFD-fed C57BL/6 mice increased local expression of many cytokines and receptors in the GH/IGF-I pathways, including *GH-R*, *IGF-I*, *IGF-II*, *IGF-IR*, *PRLR*, *Sst1*, *Sst2*, *Sst4*, but no local expression of GH was identified in the mammary glands [122]. It is suggested systemic GH may act on GF-R and stimulate IGF-I, and thus modulate mammary development via autocrine or paracrine pathways [122]. Genetically engineered mice with increased endogenous GH show further increased tumor incidence only in HFD-fed mice, but not LFD-fed controls, supporting a role of the GH and IGF-I pathways in regulating HFD-mediated tumor promotion [25].

HFD promotion of tumorigenesis is hypothesized to be partially mediated by inflammatory processes involving macrophages [26, 28]. Intratumoral macrophages have been correlated with high histological grade, epithelial-mesenchymal transition, and poor breast cancer disease-free survival [123], and gathers great interest as a potential target for cancer therapy. HFD can recruit macrophages to the mammary epithelium. In ovariectomized C57BL/6 mice, HFD exposure from 5 weeks of age onward resulted in a significant increase in macrophage infiltration with formation of crown-like structures around adipocytes in adult mammary glands, increased MCP-1, a chemokine that recruits macrophages, and increased NF-kB activation [124]. In BALB/c mice, 3 weeks of HFD resulted in elevated *Il4* RNA levels, which could potentially stimulate M2-type macrophage differentiation [26]. Results from the current studies showed that HFD altered the inflammatory microenvironment with increased numbers of M2-type macrophages recruited to hyperplastic lesions and mammary tumors in both BALB/c and FVB mice. For the first time, we identified that alterations from pubertal HFD (HFD-LFD) were sustained to recruit increased M2-type macrophages to tumors. In the 4T1 transplantation model for metastasis, HFD also increased intratumoral M2-type macrophages with upregulation of *MCP-1, M-CSF, Ccr2, M-CSFR* [125].

We took advantage of two distinct tumor models with different modes of tumor initiation, tumor latency and vastly different tumor histological profiles. In the DMBA model, HFD promoted predominantly adenosquamous tumors. In the *Trp53*-null model, adult HFD (LFD-HFD) specifically increased spindle cell tumors. Furthermore, work from our lab has identified pubertal HFD as sufficient and

required for enhanced tumorigenesis in the DMBA model [29]. In contrast, there may or may not be two different windows of susceptibility to HFD in the *Trp53*-null model. This highlights the idea that tumor promotion by HFD is dependent on the specific tumor initiating agents and progression pathways. The majority of tumors from either model were ER-negative and PR-negative, whereas, the majority of human tumors are ER+ and/or PR+. However, more ER- and PR- tumors are found in premenopausal women [126]. These models may thus be most pertinent to the development of triple negative and basal-like breast cancers in premenopausal women. Future work is needed to investigate the role of HFD in models for ER+ and/or PR+ breast cancer.

Immunohistochemical analysis allowed for specific analysis of proliferation, angiogenesis, and selected immune microenvironment characteristics in HFD tumors. A global microarray analysis of the tumors on different dietary regimens may reveal pathways that are distinctively impacted by HFD. It may provide clues to what factors were responsible for the recruitment of the M2-type macrophages and what factors mediated the enhanced proliferation and angiogenesis by HFD. It may also shed light about how HFD in the pubertal window or the adult window differentially impact tumor pathways.

Unexpectedly, in the FVB DMBA model, we found fewer mice exhibiting hyperplastic lesions at 16 weeks on diet than at 10 weeks on diet. The mechanisms for the disappearance of these lesions are intriguing. In contrast to intratumoral macrophages, the majority of which are M2-type, a high proportion of the

hyperplasia-associated macrophages were M1-type. It remains to be determined if they are involved in resolution of lesions. It will be advantageous if we can harness and exploit the innate mechanisms for tumor surveillance as novel preventative and therapeutic strategies.

Data from these studies illuminated the detrimental effects of HFD in preclinical breast cancer models. Importantly, HFD promoted tumors independent of the development of overt obesity, and in both puberty and adulthood. It affirmed another reason to eat a balanced diet throughout one's life. However, behavioral changes can be one of the most difficult tasks in health promotion. Education and encouragement from health care professionals are typically ineffective. Recognizing that HFD may be difficult to avoid for some, further understanding of how HFD contributes to breast cancer risk are required for developing prevention strategies to alleviate the effects of HFD in high-risk individuals.

APPENDIX

Figure 2.1. Kaplan-Meier survival curves for mammary (a) tumor-specific survival and (b) overall survival in FVB mice fed a pubertal initiated LFD or HFD since 3 weeks of age. Four weekly doses of 50mg/kg DMBA were administered via oral gavage from 5 weeks of age to initiate tumors. HFD significantly increased DMBA-induced mammary tumor incidence and decreased their latency ($p<0.01$). HFD also significantly increased the incidence of many other types of tumors, including skin tumors, lymphomas, thymomas and hepatic tumors, resulting in poorer overall survival ($p<0.01$).

(a)

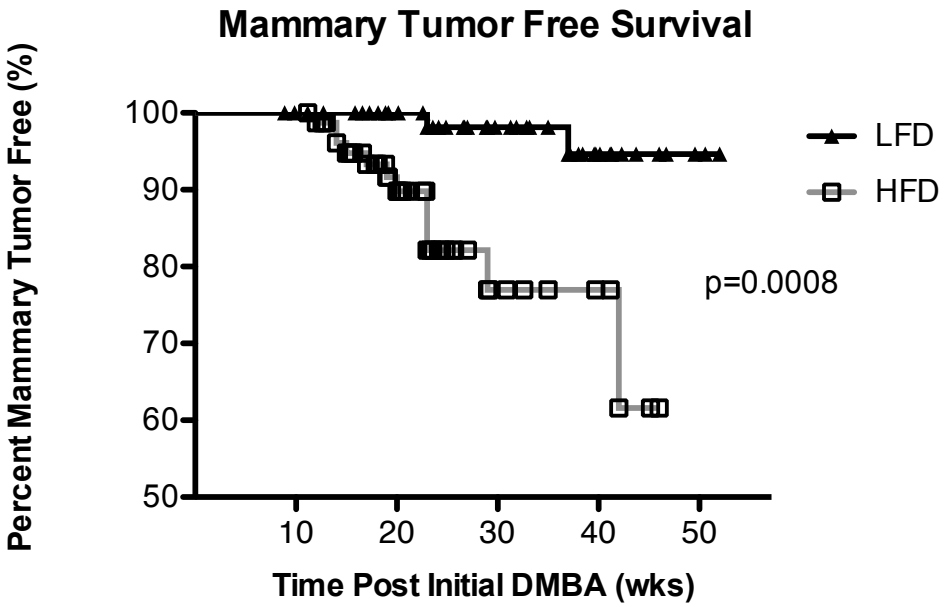

(b)

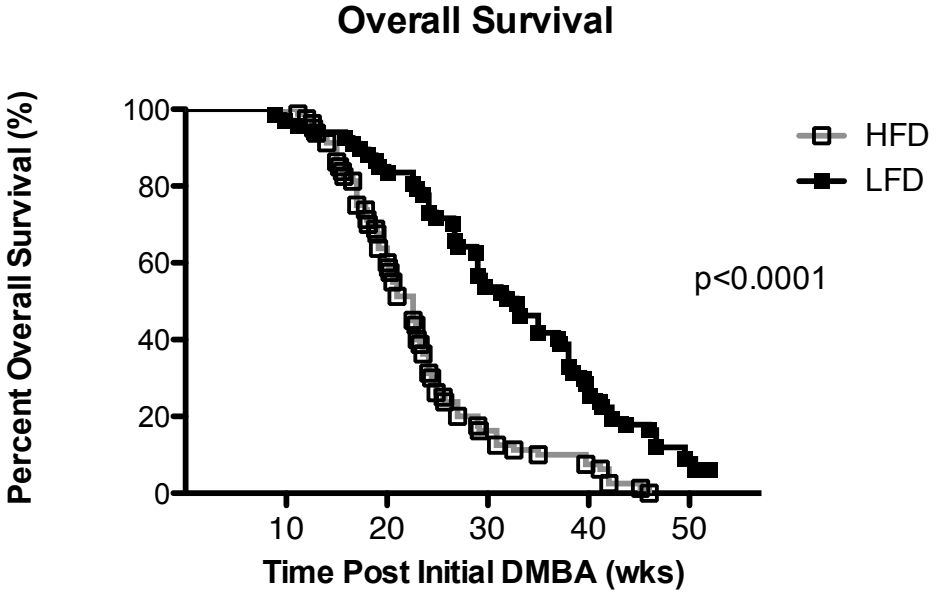

Figure 2.2. Macrophage recruitment in DMBA-induced tumors. (a), Arg1-, M1-type of macrophages are predominant in the periphery and the center of tumors from both LFD and HFD-fed mice. (b), Higher proportion of M2-type macrophages were found in the center of HFD tumors (16% HFD vs. 4% LFD). (n=1 for LFD Tumor Edge, n=2 for LFD Tumor Center; n=6 for HFD Tumor Edge, n=8 for HFD Tumor Center).

(a)

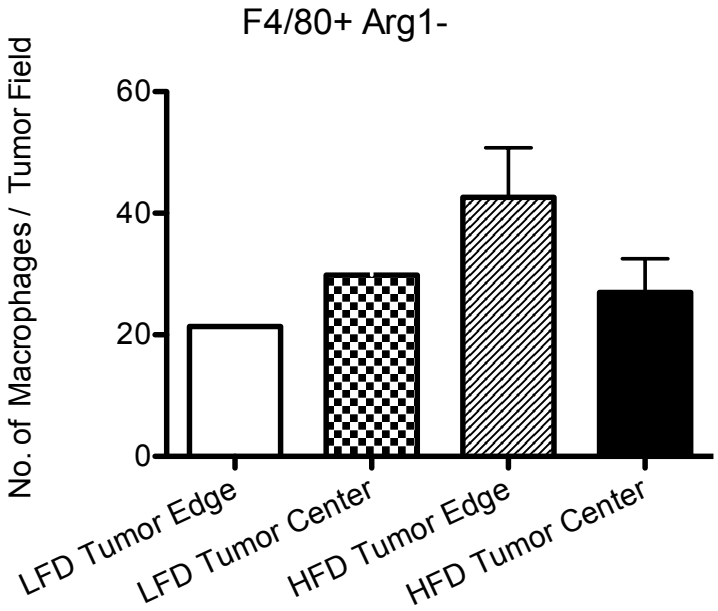

(b)

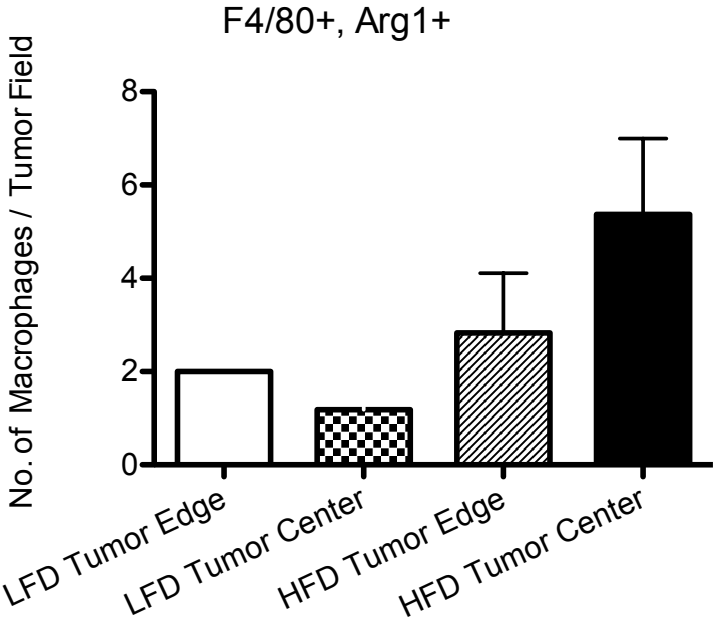

Figure 2.3. Pubertal mammary gland characteristics in FVB mice on LFD or HFD. (a), Number of terminal end buds (TEBs) in pubertal mice fed either a LFD or HFD. (*, $p<0.05$, n=5 for each group.) (b), Ductal elongation in pubertal mice fed either a LFD or HFD. (*, $p<0.05$, n=5 for each group).

(a)

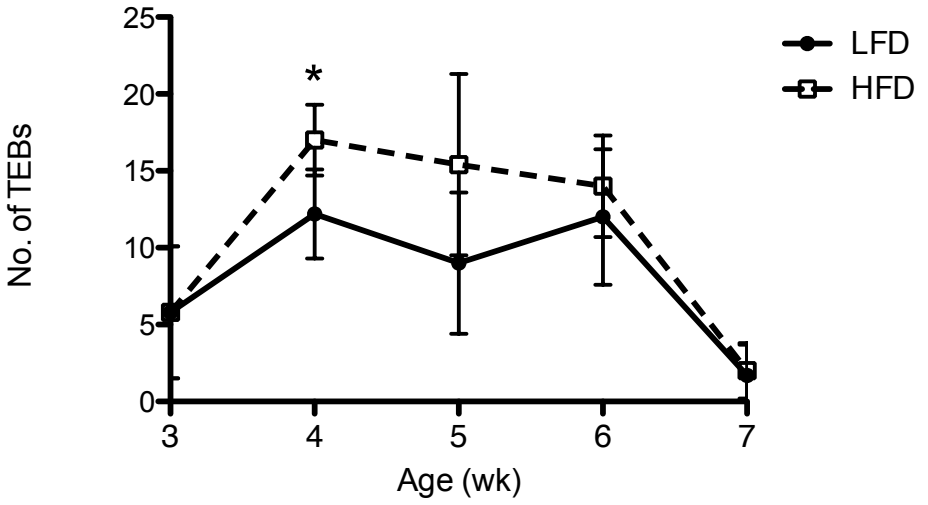

(b)

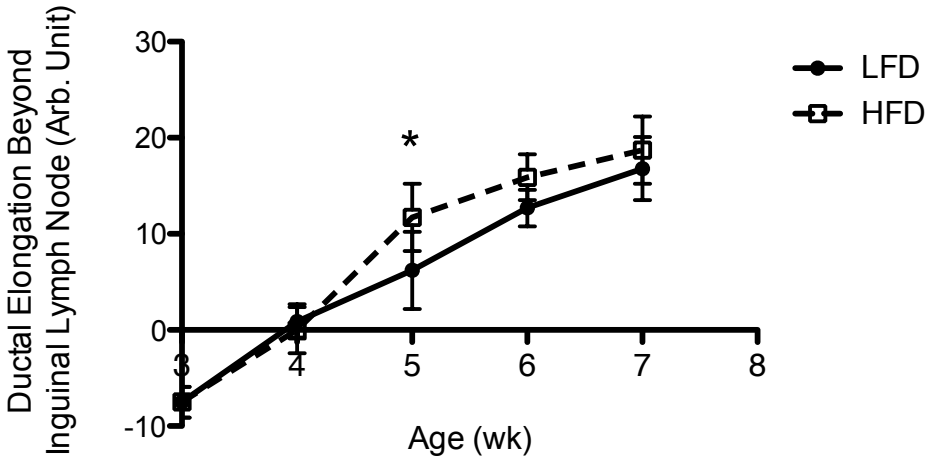

Figure 2.3 (cont'd). (c), Representative whole mount images of mammary glands after 2 weeks on diet at 5 weeks of age. Lines indicate the distal edge of the mammary ductal tree.

(c)

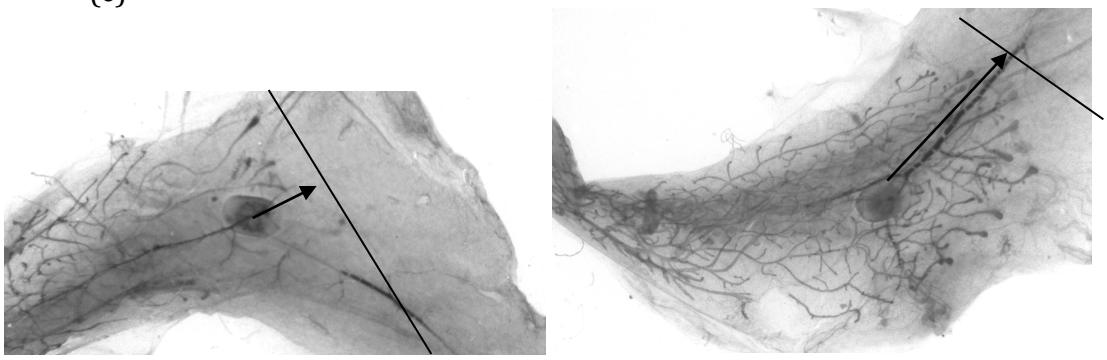

LFD HFD

Figure 2.4. Cellular proliferation after 2 weeks on diet. HFD significantly increased the proportion of proliferating cells in large ducts, small ducts and TEBs after 2 weeks on diet, and no differences were observed after 4 weeks on diet. (*, $p<0.05$, n=5 for each group).

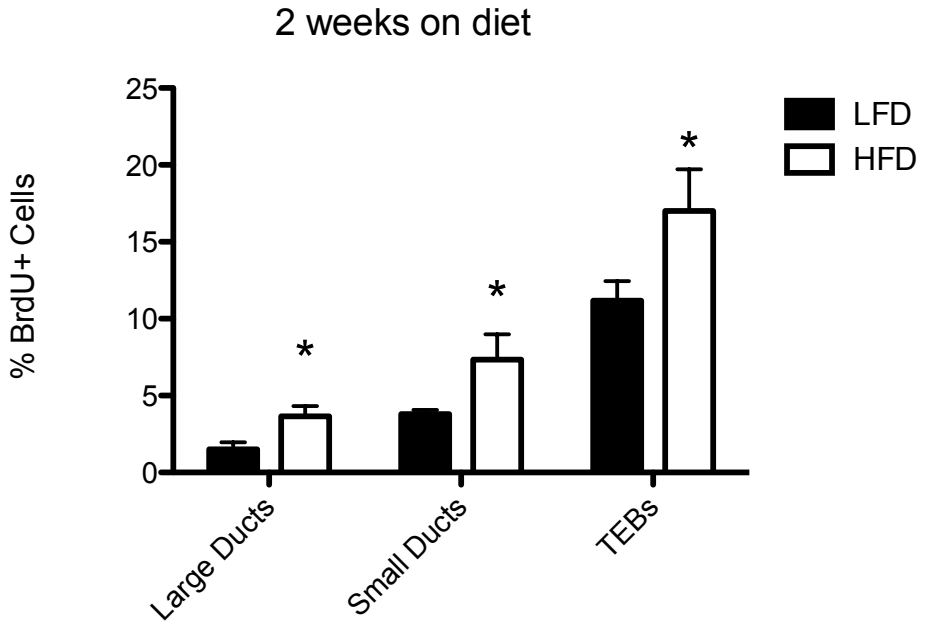

Figure 2.5. Hyperplastic lesions in mammary glands no. 2 and 3 at 10 and 16 weeks on diet. After 10 weeks on diet, a trend of more lesions were observed in HFD-fed mice (p=0.12, n=10). By 16 weeks of diet, the number of hyperplastic lesions in LFD and HFD-fed mice was similar (n=6).

(a)

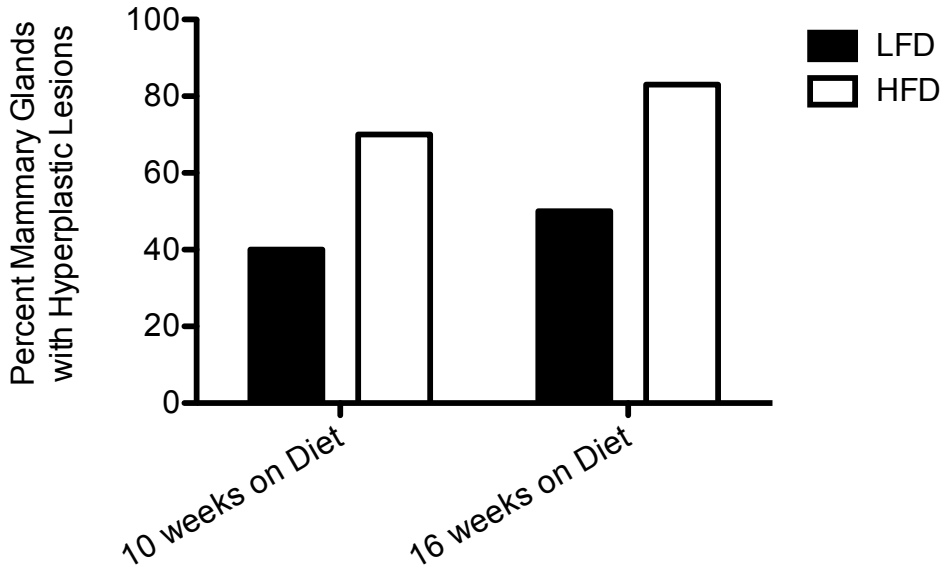

(b)

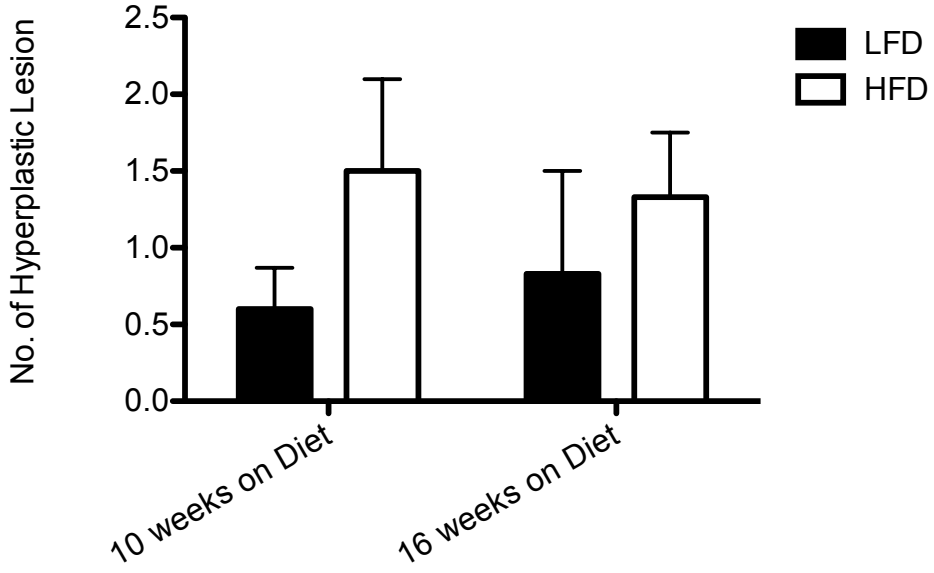

Figure 2.6. Macrophage recruitment at 10 weeks and 16 weeks on diet. (a), HFD did not change the number of macrophages associated with normal structures. After 10 weeks on diet, HFD significantly recruited more Arg1- M1-type of macrophages (p=0.01), while the change in the number of Arg1+ M2-macrophages were not statistically significant (p=0.2). (n=5 for each group).

(a)

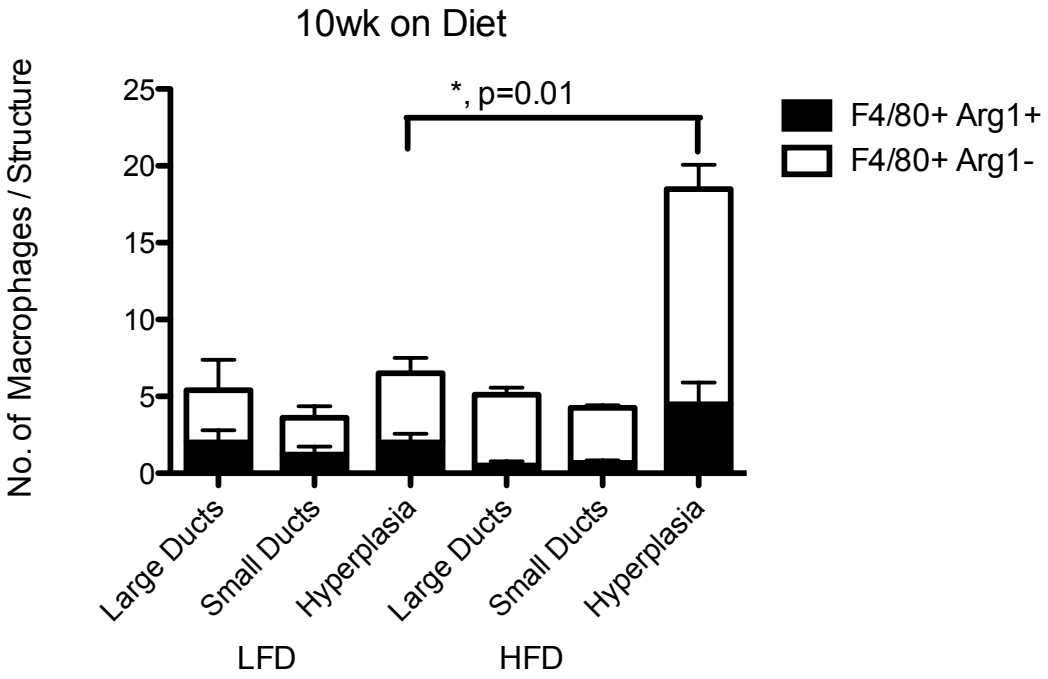

Figure 2.6 (cont'd). (b), After 16 weeks on diet, the recruitment of both Arg1- M1 and Arg1+ M2 macrophages remained elevated by HFD. (p=0.2 and p=0.07 for M1 and M2-type, respectively). (n=5 for each group).

(b)

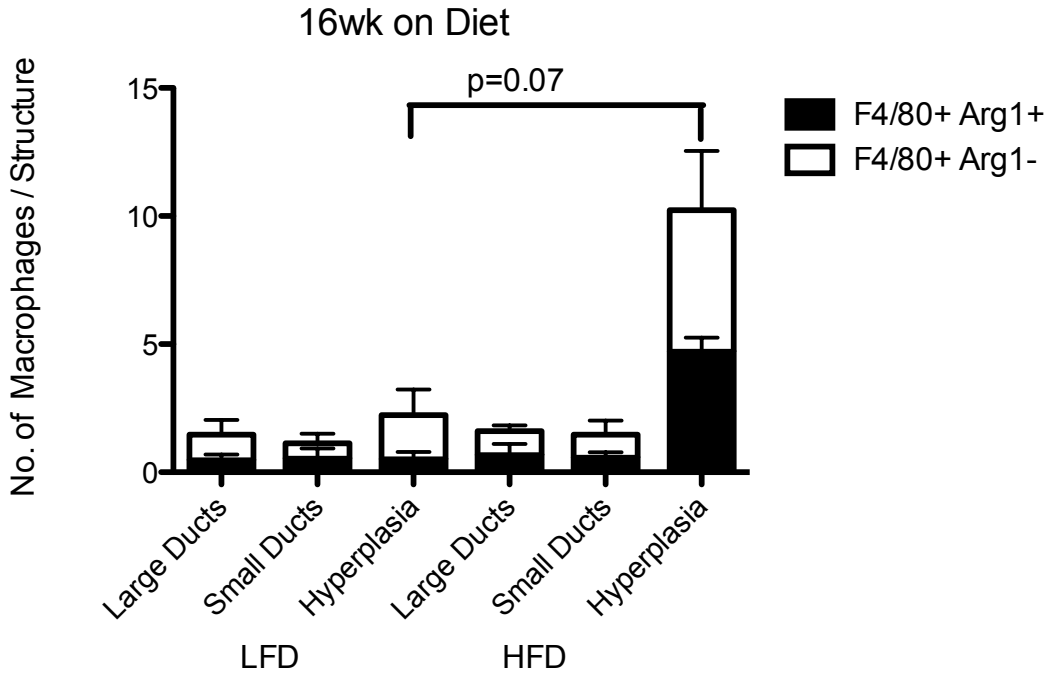

Figure 2.7. Weight gain in DMBA-treated FVB mice on either LFD or HFD. (b), After 10 days on diet (31 days of age), pubertally initiated HFD at 3 weeks of age promoted increased body weight gain. HFD initiated from 3 weeks of age increased pubertal body weight gain between 4.4 to 8 weeks of age. (a), The pubertal gain was lost in mice on HFD after DMBA exposures. Mice on HFD regained their lost weight and become heavier than controls by 17 weeks of age in adulthood. By the end of the body weight measurement at 40 weeks of age, mice on HFD were 24% heavier than their LFD counterparts. (n>8 in all data points).

(a)

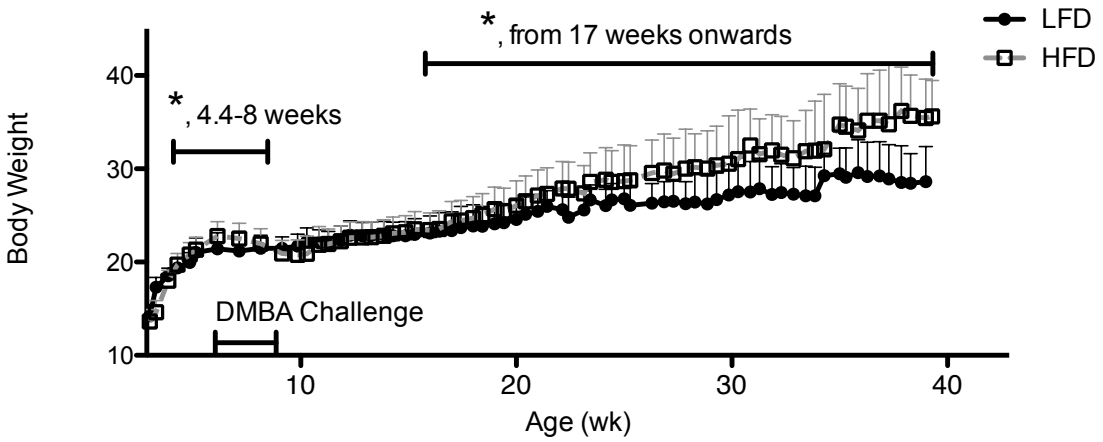

(b)

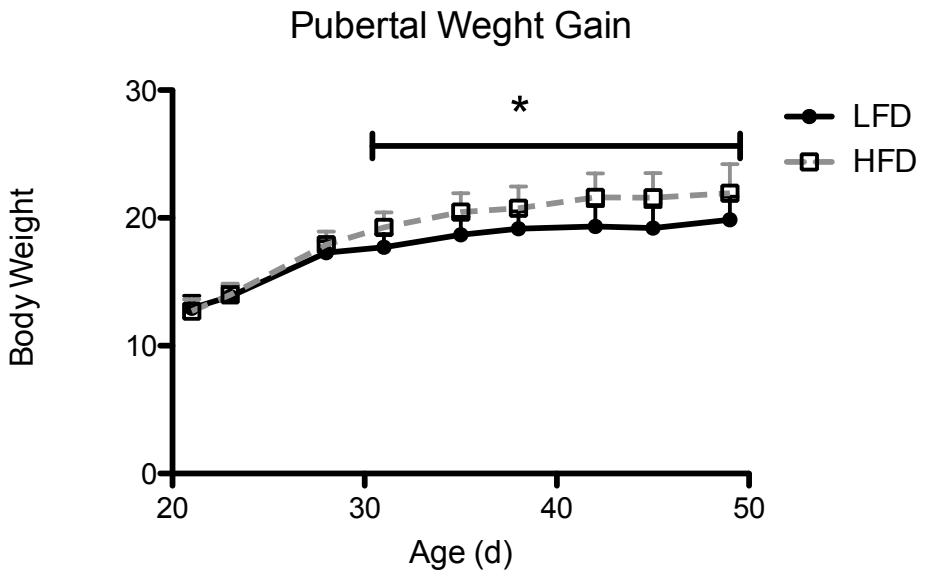

Figure 2.8. Fasting plasma glucose and insulin levels at 10 and 16 weeks on diet. (a), Fasting plasma glucose levels were increased in HFD-fed animals after 16 weeks on diet. (b), At a younger age, after 10 weeks on diet, LFD-fed mice had higher fasting insulin levels. High variance was observed in fasting plasma insulin levels among mice in the same treatment groups at later time points, possibly due to DMBA-associated pathology.

(a)

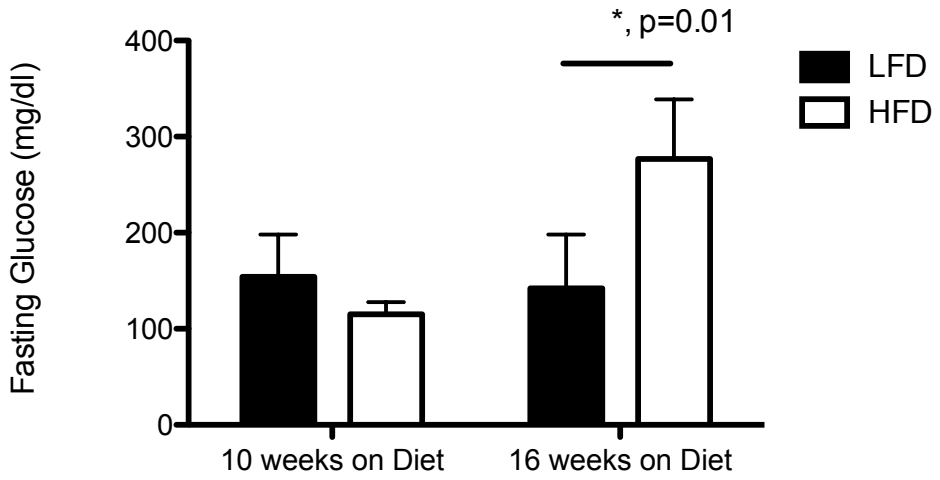

(b)

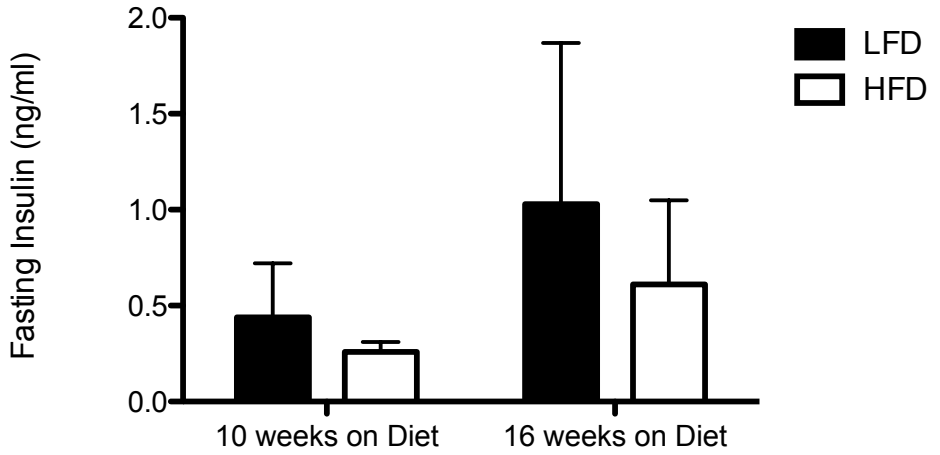

Table 2.1. Diet compositions.

Ingredients (g/100g)		**Low Fat Diet (LFD)**	**High Fat Diet (HFD)**
Fat	Corn Oil	2.369	16.1498
	Lard	1.8957	31.6537
Carbohydrate	Corn Starch	54.407	8.89
	Maltodexdrin	11.848	16.1498
Protein	Casein	18.987	25.8397
	L-cystine	0.2843	0.3876
Fiber	Cellulose	4.7393	6.4599
Vitamins	Vitamin Mix V10001	0.9479	1.2919
	Choline Bitartrate	0.1896	0.2584
Minerals	Mineral Mix S10026	0.9479	0.1286
	Dicalcium Phosphate	1.2322	1.6795
	Calcium Carbonate	0.5213	0.7106
	Potassium Citrate, 1 H_2O	1.5639	2.1318
Energy			
kcal density/g		3.8	5.2
% kcal	Fat	10	60
	Carbohydrate	70	20
	Protein	20	20

Table 2.2. FVB DMBA tumors used for microarray analysis.

Diet	Tumor#	Histopathology	Latency (weeks)
HFD- Early	M45	Adenosquamous	19
	M20	Adenosquamous	20
	M27	Solid	22
	M72	Glandular	24
HFD-Late	M37	Cribriform	28
	M47	Spindle Cell	28
	M80	Papillary	34
	M84	Solid	47
LFD-Late	M34	Adenosquamous	28
	M46	Cribriform	42

Figure 3.1. Experimental scheme. Fragments of *Trp53-null* mammary duct were transplanted into cleared fat pads of female 3-week-old wild-type BALB/c mice. After the surgery, mice were randomly assigned to four diet groups. Control group (n=33) were fed LFD, and continuous HFD group (n=31) were fed HFD *ad libitum*. To investigate the effects of HFD exposure during peripubertal window, a group of HFD-fed mice (n=31) were switched to LFD at 10 weeks of age. Similarly, to investigate the effects of HFD exposure during the adult window, a group of LFD-fed mice (n=31) were switched to HFD at 10 weeks of age. Tumor development was monitored until mice reached 500 days of age.

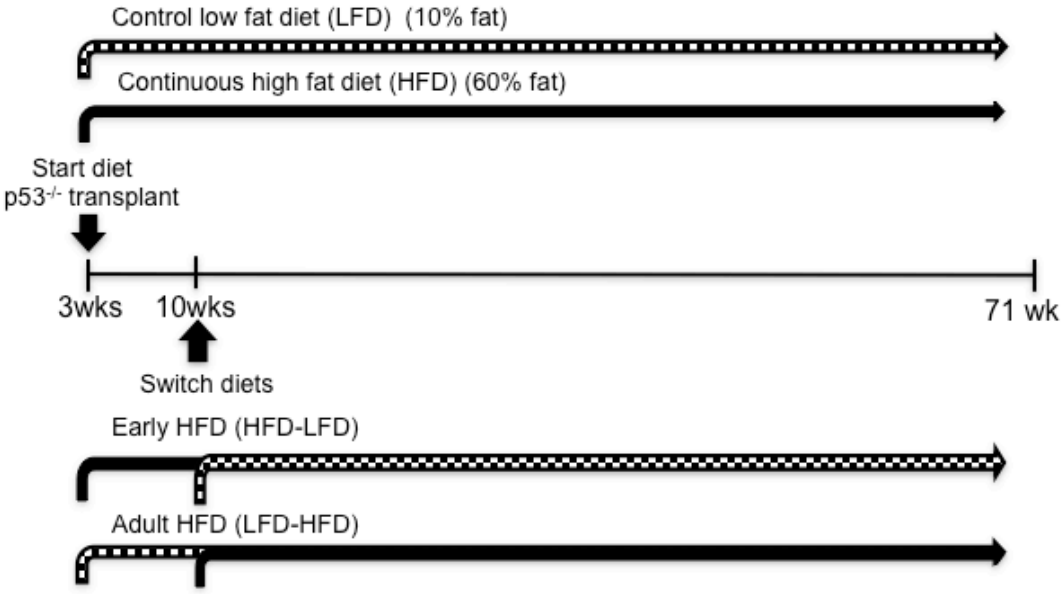

Figure 3.2. The effect of the various dietary regimens on tumor free survival. Kaplan-Meier plots were determined for BALB/c mice receiving *Trp53-null* mammary transplants fed a control lifelong low fat diet (LFD; n= 37), a lifelong high fat diet (HFD; n= 46), a peripubertal high fat diet (HFD-LFD, n=42), and a high fat diet restricted to adulthood (LFD-HFD, n=38). (a) One-year tumor free survival was significantly reduced in mice fed HFD-LFD and LFD-HFD. (Log-rank tests, LFD vs. HFD, p = 0.158; LFD vs. HFD-LFD, *, p = 0.042; LFD vs. LFD-HFD, **, p = 0.009). (b) 500-day tumor free survival was significantly reduced by lifelong HFD and LFD-HFD, but not HFD-LFD. (Log-rank tests, LFD vs. HFD, *, p = 0.046; LFD vs. HFD-LFD, p = 0.131; LFD vs. LFD-HFD, **, p = 0.006).

(a)

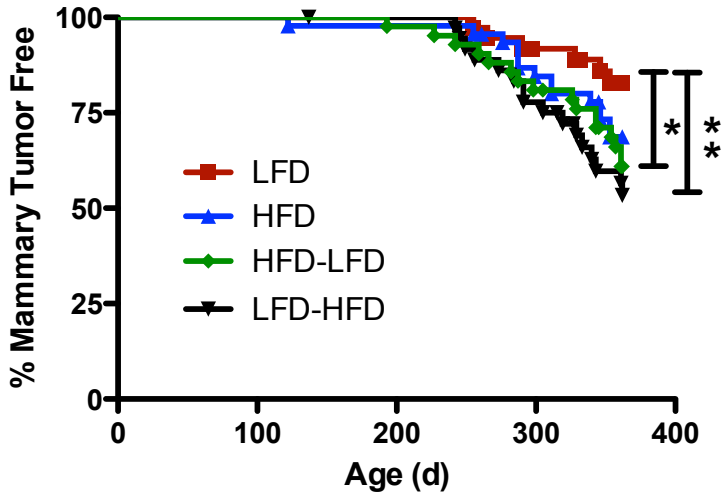

(b)

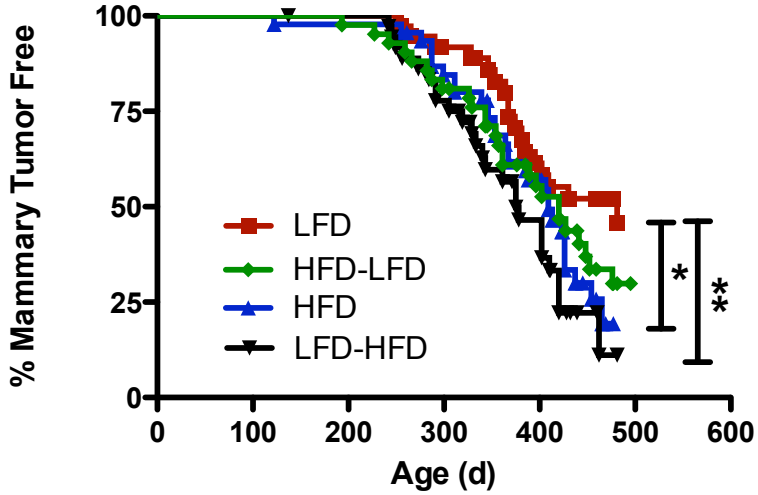

Figure 3.3. Proportions of tumors by histopathology across the different dietary regimens in BALB/c mice receiving *Trp53-null* mammary transplants. (a) LFD-HFD increased the proportion of spindle cell carcinomas by 2.7-fold compared to LFD ($p = 0.02$). (b - d) Representative H&E stained sections of epithelial, spindle cell and adenosquamous tumors. Scale bar = 0.25mm.

(a)

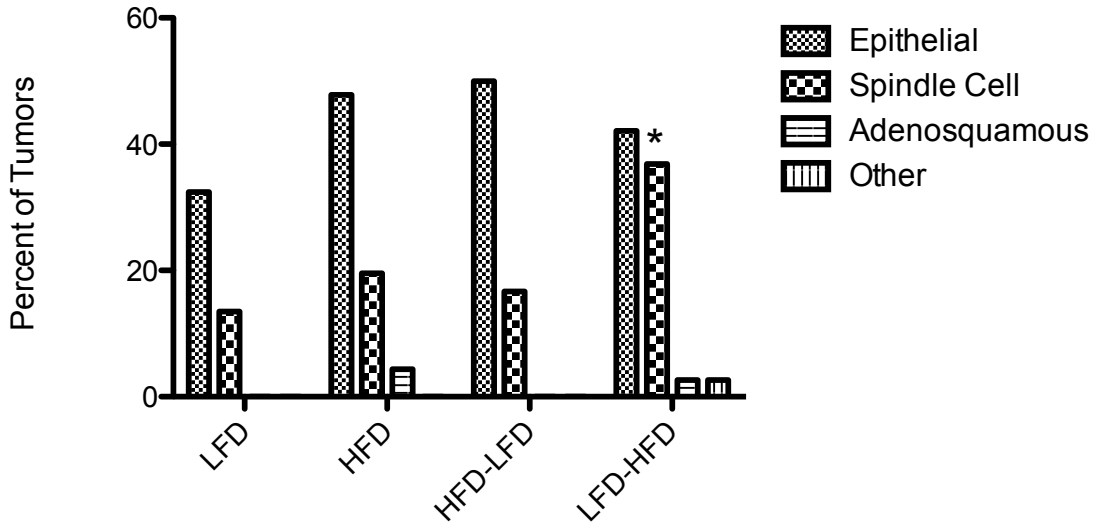

(b) Epithelial (c) Spindle Cell (d) Adenosquamous

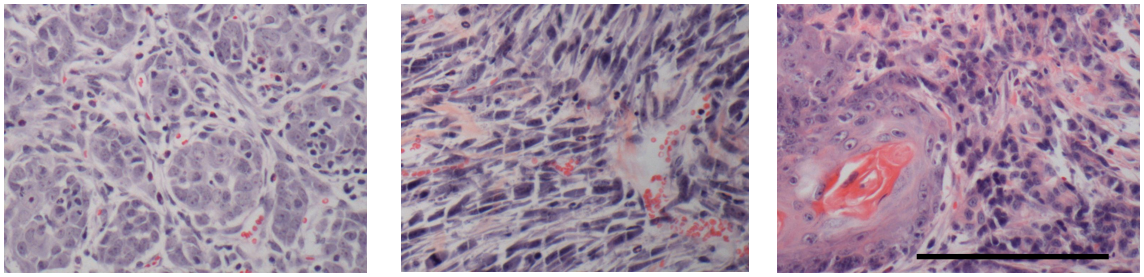

Figure 3.4. Effects of various dietary regimens on proliferation and apoptosis in *Trp53-null* tumors. (a) HFD at any life stage significantly increased proliferation marker PCNA in tumors ($p < 0.01$). (b) Lifelong HFD and LFD-HFD decreased apoptosis as measured by TUNEL labeling ($p<0.05$).

(a)

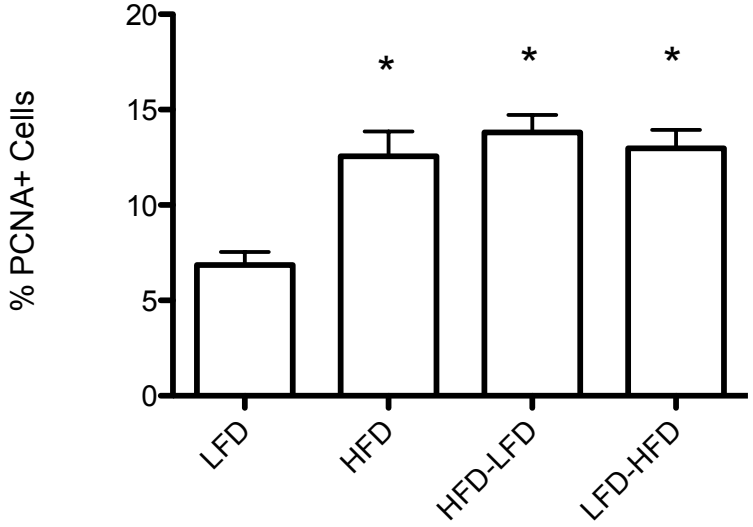

(b)

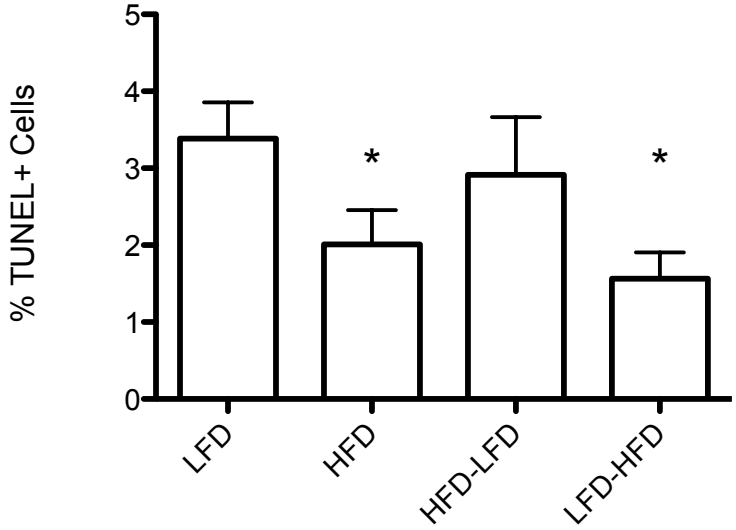

Figure 3.5. Effects of dietary regimens on tumor vascularity. HFD at any life stage increased blood vessel density in epithelial tumors (*, p<0.01). Independent of diet, spindle cell tumors had higher blood vessel density than epithelial tumors (#, p=0.01).

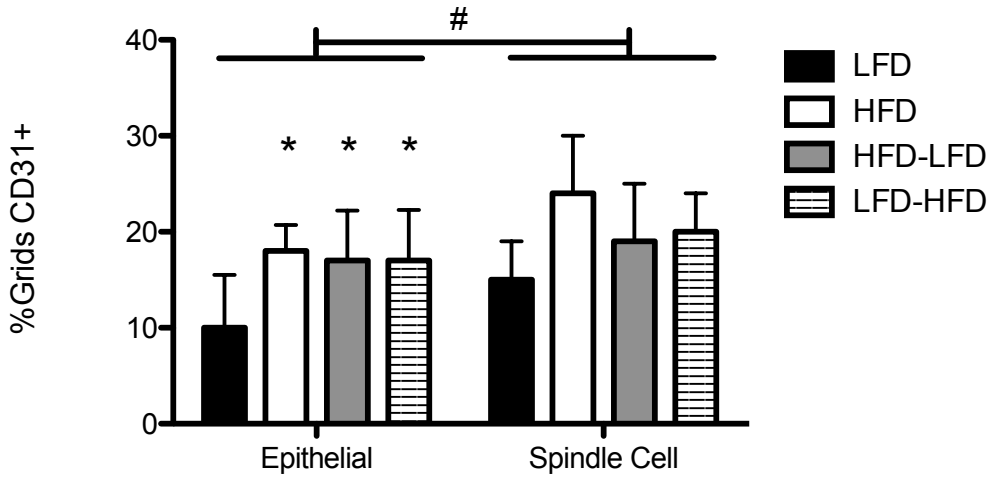

Figure 3.6. Quantitation of macrophages within tumors. HFD, HFD-LFD and LFD-HFD all increased the number of Arg1+, M2 macrophages and the number of total macrophages within tumors (*, **, $p<0.05$).

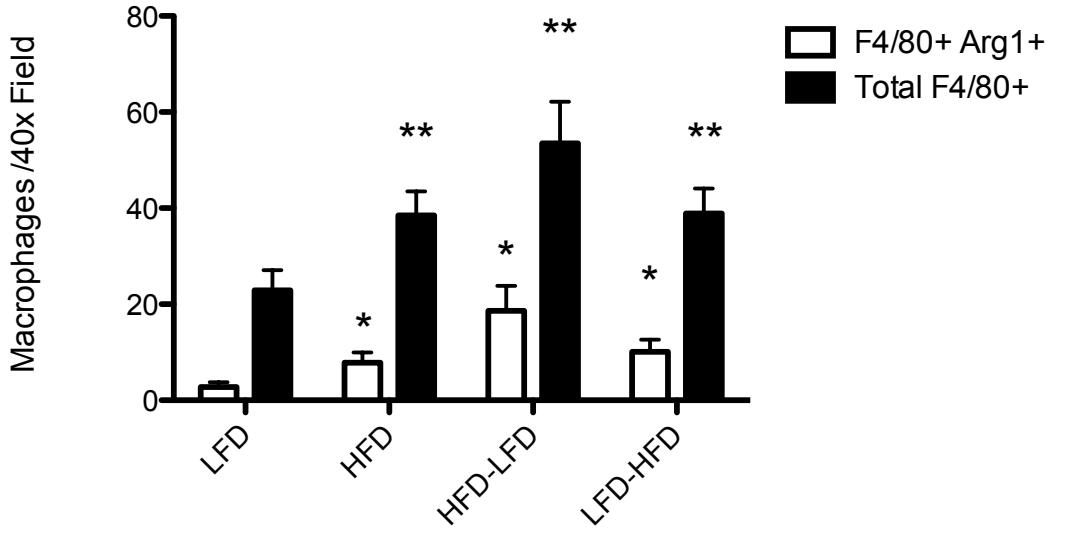

Figure 3.7. Body weight over time. Mice fed lifelong HFD had increased body weight compared to mice fed lifelong LFD after 7 weeks on diet, while mice fed adulthood restricted HFD (LFD-HFD) had increased body weight 7 weeks after diet switch to HFD. Mice fed a peripubertal HFD (HFD-LFD) had similar weights to those fed lifelong LFD. The weight gain in mice fed HFD and LFD-HFD was modest at 14±8 % and 17±9 %, respectively, by end of the experiments at 71 weeks of age.

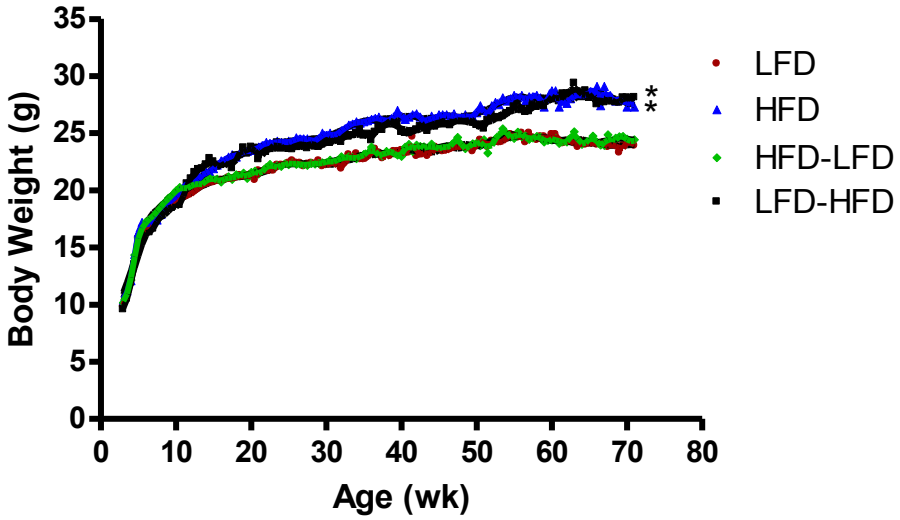

Figure 3.8. Non-fasting plasma glucose (a) and insulin (b) in tumor bearing mice. No significant differences were found in any dietary regimen.

(a)

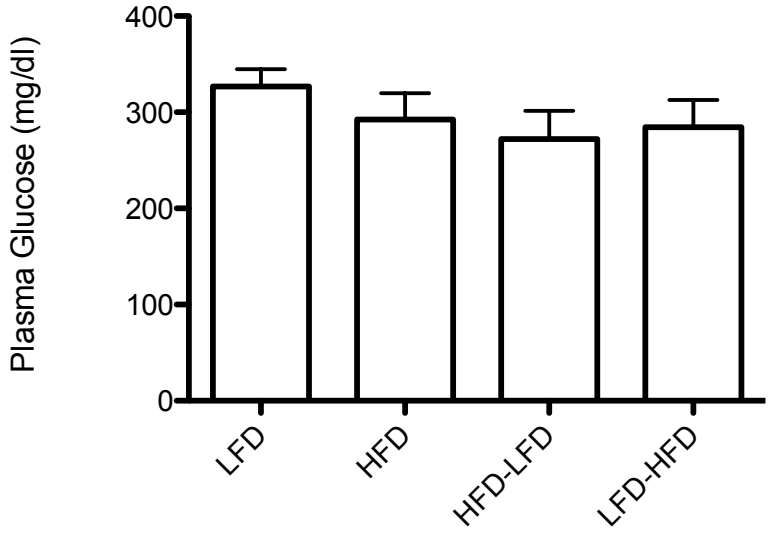

(b)

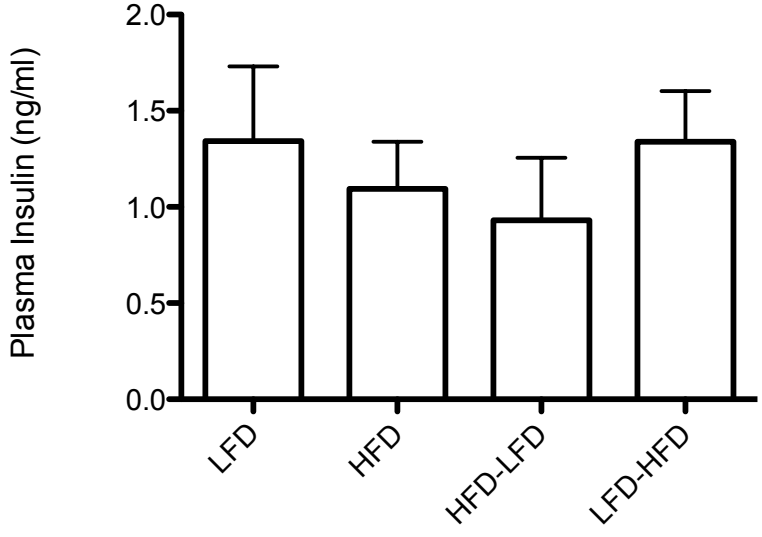

Table 3.1. BALB/c Trp53-/- tumors used for microarray analysis.

Epithelial tumors			
Diet	**Tumor#**	**Histopathology**	**Latency (weeks)**
LFD-Early	31R	Glandular	36
	22R	Cribriform	38
	17R	Cribriform	41
	11R	Cribriform	47
LFD-Late	13L	Solid	53
	19R	Glandular	54
	27L4A	Glandular	56
	11L	Cribriform	58
HFD-Early	42L4B	Cribriform	40
	60L	Cribriform	41
	65R	Cribriform	41
	40R4A	Glandular	44
HFD-Late	57R	Cribriform	52
	66L	Papillary	55
	56R	Cribriform	55
	62L	Glandular	59
LFD-HFD-Early	80L	Cribriform	35
	92R	Cribriform	36
	78R	Cribriform	42
	82L	Glandular	48
LFD-HFD-Late	71L	Cribriform	52
	101R	Cribriform	57
	101L4A	Papillary	57
	90R	Cribriform	60
HFD-LFD-Early	117L	Cribriform	35
	115R	Cribriform	37
	117R	Cribriform	40
	107L	Cribriform	43
HFD-LFD-Late	108R	Glandular	56
	109L	Cribriform	57
	110R	Cribriform	60
	122R	Glandular	60

Table 3.2. Proportion of ER+/PR+ tumors by diet treatments and histopathology.

Diet	Tumor Type	ER+PR+/Total
LFD	Epithelial	3/12
	Spindle Cell	0/5
HFD	Epithelial	8/26
	Spindle Cell	0/8
LFD-HFD	Epithelial	5/19
	Spindle Cell	0/12
HFD-LFD	Epithelial	5/21
	Spindle Cell	0/8

Table 3.3. List of significant differentially upregulated canonical pathways and molecular functions in early occurring tumors (latency less than 48 weeks) compared to late occurring tumors.

Canonical Pathway

Canonical Pathway	B-H Adjusted p-value	Ratio
Interferon Signaling	3.03E-02	2/29
Activation of IRF by Cytosolic Pattern Recognition Receptors	4.49E-02	2/50

Molecular Functions

Categories	Functions	B-H Adjusted p-Value	Molecules	No. of Molecules
Cell Death and Survival	killing of cells	6.75E-03	ADAR, ITGAE, LY9	3
Cell Morphology	morphology of leukocytes	5.53E-03	ADAR, CCR9, IL2RB, Irgm1, LY9	5
Cell Morphology, Hematological System Development and Function	abnormal morphology of T lymphocytes	8.06E-03	CCR9, IL2RB, LY9	3
Cell-mediated Immune Response, Cellular Development, Cellular Function and Maintenance, Hematological System Development and Function, Hematopoiesis, Lymphoid Tissue Structure and Development	T cell development	3.07E-03	CCR9, CD69, IL2RB, LY9, RSAD2, STAT2	6
	differentiation of T lymphocytes	4.49E-03	CCR9, CD69, IL2RB, RSAD2, STAT2	5
Cell-mediated Immune Response, Cellular Movement, Hematological System Development and Function, Immune Cell Trafficking	cell movement of T lymphocytes	3.12E-03	CCR9, CD69, CXCL10, ITGAE	4
	homing of T lymphocytes	3.12E-03	CCR9, CXCL10, ITGAE	3
Cell-To-Cell Signaling and Interaction, Cellular Movement, Hematological System Development and Function, Immune Cell Trafficking	recruitment of leukocytes	3.32E-02	CD69, CXCL10, ITGAE	3

Table 3.3 (cont'd).

Cellular Development	differentiation of cells	3.88E-02	ADAR, CCR9, CD69, CXCL10, HERC6, IL2RB, RSAD2, STAT2	8
Cellular Development, Cellular Growth and Proliferation, Hematological System Development and Function	proliferation of T lymphocytes	9.97E-03	CD69, IL2RB, Irgm1, LY9, Slfn1	5
Cellular Development, Hematological System Development and Function	differentiation of blood cells	4.45E-03	ADAR, CCR9, CD69, HERC6, IL2RB, RSAD2, STAT2	7
Cellular Development, Hematological System Development and Function, Hematopoiesis	differentiation of leukocytes	6.46E-03	ADAR, CCR9, CD69, IL2RB, RSAD2, STAT2	6
	development of hematopoietic progenitor cells	1.39E-02	ADAR, CCR9, IL2RB	3
Cellular Development, Hematological System Development and Function, Hematopoiesis, Lymphoid Tissue Structure and Development	development of leukocytes	2.02E-03	ADAR, CCR9, CD69, IL2RB, LY9, RSAD2, STAT2	7
Cellular Function and Maintenance	cellular homeostasis	6.46E-03	CCR9, CD69, Iigp1, IL2RB, Irgm1, LY9, RSAD2, STAT2	8
Cellular Movement	chemotaxis of cells	3.48E-02	CCR9, CD69, CXCL10	3
Cellular Movement, Hematological System Development and Function, Immune Cell Trafficking	cell movement of leukocytes	2.56E-03	CCR9, CD69, CXCL10, IL2RB, Irgm1, ITGAE, STAT2	7
	homing of leukocytes	6.75E-03	CCR9, CD69, CXCL10, ITGAE	4
	cell movement of myeloid cells	2.10E-02	CD69, CXCL10, IL2RB, Irgm1	4
	cell movement of granulocytes	3.67E-02	CD69, CXCL10, IL2RB	3
Connective Tissue Disorders, Inflammatory Disease, Skeletal and Muscular Disorders	arthritis	3.37E-02	CD69, IL2RB, Slfn1	3
Embryonic Development, Organ Development, Organismal Development	development of lymphatic system	4.89E-02	ADAR, CCR9, IL2RB	3

Table 3.3 (cont'd).

Endocrine System Disorders, Gastrointestinal Disease, Immunological Disease, Metabolic Disease	insulin-dependent diabetes mellitus	5.19E-14	CCR9, CXCL10, GBP6, Gbp8, HERC6, Ifi47, IFIT1B, Iigp1, IL2RB, Irgm1, ITGAE, STAT2, Tgtp1/Tgtp2	13
Hematological System Development and Function, Hematopoiesis, Lymphoid Tissue Structure and Development, Organ Morphology, Tissue Morphology	quantity of thymocytes	6.75E-03	CCR9, IL2RB, LY9, Slfn1	4
Hematological System Development and Function, Hematopoiesis, Tissue Morphology	quantity of hematopoietic progenitor cells	3.07E-03	CCR9, CD69, IL2RB, Irgm1, LY9, Slfn1	6
Hematological System Development and Function, Humoral Immune Response, Tissue Morphology	quantity of B lymphocytes	4.80E-02	CCR9, CD69, IL2RB	3
Hematological System Development and Function, Tissue Morphology	quantity of T lymphocytes	2.15E-03	CCR9, CD69, CXCL10, IL2RB, ITGAE, LY9, Slfn1	7
	morphology of bone marrow	5.99E-03	ADAR, IL2RB, Irgm1	3
	quantity of blood cells	6.75E-03	CCR9, CD69, CXCL10, IL2RB, Irgm1, ITGAE, LY9, Slfn1	8
	quantity of CD4+ T-lymphocytes	1.35E-02	CD69, CXCL10, IL2RB	3
Humoral Immune Response, Protein Synthesis	quantity of IgG	6.75E-03	CD69, CXCL10, IL2RB, RSAD2	4
Immunological Disease	systemic autoimmune syndrome	5.19E-14	CCR9, CXCL10, GBP6, Gbp8, HERC6, Ifi47, IFIT1B, Iigp1, IL2RB, Irgm1, ITGAE, Slfn1, STAT2, Tgtp1/Tgtp2	14
Infectious Disease	infection of mammalia	2.02E-03	CXCL10, Ifi47, Iigp1, Irgm1, ITGAE, STAT2	6
	viral infection	6.75E-03	ADAR, CXCL10, RSAD2, STAT2	4
	parasitic infection	9.97E-03	Ifi47, Iigp1, Irgm1	3
Protein Synthesis	quantity of interferon	2.56E-03	ADAR, Irgm1, RSAD2	3

Table 3.4. List of significant differentially regulated canonical pathways and molecular functions in early occurring epithelial tumors (latency less than 48 weeks) compared to late occurring epithelial tumors.

Down-Regulated

Molecular Functions

Categories	Functions	B-H Adjusted p-Value	Molecules	No. of Molecules
Antimicrobial Response, Inflammatory Response	antiviral response	1.58E-03	IFIT1B, IFIT2, IFITM3, IL12B	4
Cellular Movement, Hematological System Development and Function, Immune Cell Trafficking	cell movement of myeloid cells	4.68E-02	CCL25, IL12B, IL2RB, Irgm1	4
Cellular Movement, Hematological System Development and Function, Immune Cell Trafficking, Inflammatory Response	cell movement of macrophages	4.15E-02	CCL25, IL12B, Irgm1	3
Endocrine System Disorders, Gastrointestinal Disease, Immunological Disease, Metabolic Disease	insulin-dependent diabetes mellitus	2.89E-05	GBP6, IFIT1B, IFIT2, IL12B, IL2RB, Irgm1, RNASE6, Trim30a/Trim30d	8
Inflammatory Response	inflammation of intestine	4.68E-02	CCL25, IL12B, PIP	3
Lymphoid Tissue Structure and Development, Organ Morphology, Tissue Morphology	abnormal morphology of lymph node	3.32E-02	CCL25, IL2RB, PIP	3

Up-Regulated

Canonical Pathways

Canonical Pathways	B-H Adjusted p-value	Ratio	Molecules
Activation of IRF by Cytosolic Pattern Recognition Receptors	1.59E-03	5/50	DHX58, IRF7, STAT2, STAT1, ADAR
Retinoic acid Mediated Apoptosis Signaling	9.41E-03	4/44	PARP10, Ifnz (includes others), TNFSF10, PARP14

Table 3.4 (cont'd).

Pathogenesis of Multiple Sclerosis	2.42E-02	2/6	CXCL10, CCR5
Interferon Signaling	2.42E-02	3/29	IFIT1, STAT2, STAT1
Role of Lipids/Lipid Rafts in the Pathogenesis of Influenza	3.65E-02	2/9	RSAD2, Ifnz (includes others)
Tec Kinase Signaling	4.41E-02	5/148	ITGA3, VAV3, TNFSF10, STAT2, STAT1

Molecular Functions

Categories	Functions	B-H Adjusted p-Value	Molecules	No. of Molecules
Antimicrobial Response, Inflammatory Response	antimicrobial response	4.06E-03	Defa3 (includes others), DHX58, IRF7, Mx1/Mx2, RSAD2, SLAMF8, STAT1	7
	antiviral response	5.59E-03	DHX58, IRF7, Mx1/Mx2, RSAD2, STAT1	5
Cell Death and Survival	killing of cells	2.13E-02	ADAR, CCR5, ITGAE, STAT1, TNFSF10	5
Cell Signaling	replication of viral replicon	4.06E-03	ADAR, Mx1/Mx2, RSAD2	3
Cellular Development, Skeletal and Muscular System Development and Function, Tissue Development	differentiation of myoblasts	3.19E-02	CXCL10, Cxcl9, Prl2c2 (includes others), STAT1	4
Cellular Function and Maintenance, Hematological System Development and Function	function of T lymphocytes	4.51E-02	CCR5, CXCL10, HSH2D, IRF7, NLRC5, TNFSF10, Trim30a/Trim30d	7
	function of lymphocytes	4.52E-02	CCR5, CXCL10, HSH2D, IRF7, NLRC5, STAT1, TNFSF10, Trim30a/Trim30d	8
Endocrine System Disorders, Gastrointestinal Disease, Immunological Disease, Metabolic Disease	insulin-dependent diabetes mellitus	8.51E-14	CCR5, CXCL10, Cxcl9, GBP6, Gbp8, Gm5431, HERC6, HPSE, IFI16, IFI44, Ifi47, Iigp1, IRF7, ITGAE, PARP14, STAT1, STAT2, Tgtp1/Tgtp2, TNFSF10, TNFSF8, Trim30a/Trim30d	21
Endocrine System Disorders, Gastrointestinal Disease, Metabolic Disease	diabetes mellitus	9.18E-13	CCR5, CXCL10, Cxcl9, GBP6, Gbp8, Gm5431, HERC6, HPSE, IFI16, IFI44, Ifi47, Iigp1, IRF7, ITGAE, LGALS9B, PARP14, STAT1, STAT2, Tgtp1/Tgtp2, TNFSF10, TNFSF8, Trim30a/Trim30d	22

Table 3.4 (cont'd).

Hematological Disease	toxemia	1.94E-02	CCR5, CXCL10, Cxcl9, STAT1, Trim30a/Trim30d	5
Immunological Disease	systemic autoimmune syndrome	9.18E-13	CCR5, CXCL10, Cxcl9, GBP6, Gbp8, Gm5431, HERC6, HPSE, IFI16, IFI44, Ifi47, IGFBP4, Iigp1, IRF7, ITGAE, PARP14, STAT1, STAT2, Tgtp1/Tgtp2, TNFSF10, TNFSF8, Trim30a/Trim30d	22
Infectious Disease	Viral Infection	5.46E-05	ADAR, CCR5, CXCL10, DHX58, IRF7, LGALS9B, Mx1/Mx2, RSAD2, STAT1, STAT2, TNFSF10	11
	replication of virus	2.45E-03	CCR5, CXCL10, Mx1/Mx2, RSAD2, STAT1, TNFSF10	6
	infection of mammalia	2.95E-03	BAHD1, CCR5, CXCL10, DHX58, Ifi47, Iigp1, IRF7, ITGAE, STAT1, STAT2, TNFSF10	11
	anthrax	4.06E-03	CXCL10, Cxcl9, STAT1	3
	Bacterial Infection	3.19E-02	BAHD1, CCR5, CXCL10, Cxcl9, IRF7, STAT1, TNFSF10, Trim30a/Trim30d	8
	replication of RNA virus	3.48E-02	CCR5, CXCL10, Mx1/Mx2, RSAD2	4
Infectious Disease, Respiratory Disease	infection of lung	3.19E-02	CXCL10, Cxcl9, STAT1	3
Metabolic Disease	glucose metabolism disorder	9.85E-09	BGLAP, CCR5, CXCL10, Cxcl9, GBP6, Gbp8, Gm5431, HERC6, HPSE, IFI16, IFI44, Ifi47, Iigp1, IRF7, ITGAE, LGALS9B, PARP14, STAT1, STAT2, Tgtp1/Tgtp2, TNFSF10, TNFSF8, Trim30a/Trim30d	23
Organismal Survival	survival of organism	4.52E-02	CCR5, CXCL10, Cxcl9, DHX58, IFI16, IRF7, Mx1/Mx2, RSAD2, SMN1/SMN2, STAT1, STAT2, TNFSF10	12
Protein Synthesis	quantity of interferon	1.94E-02	ADAR, DHX58, RSAD2, STAT1	4

Table 3.5. List of significant differentially upregulated canonical pathways and molecular functions in spindle tumors compared to epithelial tumors.

Up-Regulated

Molecular Functions

Categories	Functions	B-H Adjusted p-Value	Molecules	No. of Molecules
Cardiovascular System Development and Function	development of vascular system	4.33E-02	AGTR2, ANGPT2, ANGPTL4, ARAP3, ARHGEF26, BMP6, BMP7, BMPR1A, BRCA1, CAT, CCL11, Ccl2, CCNA2, CD151, Cd59a, CD81, CDH5, CDKN1A, CFLAR, CLUAP1, COL3A1, COL5A1, CRK, CTSB, CTSH, CUL7, CXADR, CXCL12, CYLD, CYP1B1, CYP26A1, DDIT3, DISP1, DLL4, E2F4, EN2, FERMT3, FES, FLT4, FZD2, FZD5, GATA2, GJA1, GNA11, GPR124, GPR4, GSK3B, Gulo, HAND1, HBEGF, HEXIM1, HEY1, HIF1A, HTATIP2, ID2, IGFBP3, IGFBP4, IL7R, INHBA, INTU, IRX1, IRX4, ITGA1, ITGAV, ITGB5, KRIT1, LECT1, LEFTY1, LRG1, LRP1, LTA, MMP13, MMP14, MMP2, MMP9, MST1R, NCSTN, NDST1, NFATC4, NOS3, NOTCH2, NR4A1, OGT, PF4, PKNOX1, PLAT, PLVAP, PLXNB1, PLXND1, POLD4, PSAP, PTGS2, PTH1R, PTPRB, PXN, RAMP1, RASIP1, RHOA, RHOB, RND1, RTN4, RXRA, S1PR3, SERPINF1, SLC11A2, SLC19A1, SLIT3, SOCS3, SOX18, SPI1, SRC, STK4, TGFB1, THBD, THBS2, TIE1, TIMP3, TIPARP, TMED2, TMEM204, TTN, TWIST1, VCL, VEGFB	124
Cardiovascular System Development and Function, Organ Morphology, Skeletal and Muscular System Development and Function	contractility of ventricular myocardium	3.14E-02	ADCY6, ATP2A2, CASQ2, HBEGF, IRX4, KLK3, LMNA, MAP3K1, MMP9, NOS3, PLAT, RXRA, TIMP3, VCL	14

Table 3.5 (cont'd).

Cell Death and Survival	cell death	1.75E-02	ABCB4, ABCE1, ADAM12, ADCYAP1, AFF1, AFP, AGAP3, AGTR2, AMPD3, ANGPTL4, ANTXR2, APBB2, ARF6, ARG1, ASNA1, ASTN1, ATF1, ATF4, ATP6V1G2, ATR, B4GALNT1, BACE1, BCKDK, BCL2L1, BGN, BMP7, BMPR1A, BNIP1, BRCA1, CADPS2, CAMK1D, CAMK2N2, CAMLG, CAPN1, CASP2, CASQ2, CAT, Ccl2, CCNA1, CD151, Cd1d2, Cd24a, Cd59a, CD74, CD79B, CDH1, CDH5, CDK19, CDKN1A, CENPJ, CFLAR, CHD8, CHI3L1, CHRNA7, CIAPIN1, Clca3a1/Clca3a2, CLCN2, CLDN4, CNP, COL5A3, COPS5, CPB2, CTF1, CTNNA1, CTSB, CTSH, CUL4A, CUL7, CXADR, CXCL12, CYLD, CYP1B1, DAPK3, DCTN2, DDIT3, DDX58, DLL4, DMD, DNAJB1, DPH1, DSG2, DUSP1, E2F2, E2F4, EEF2K, EIF2AK1, EIF4EBP1, ELF4, EMP2, EN2, FAAH, FABP1, FAM134B, FES, FKBP4, FOSL1, GABBR1, GALNT3, GAS6, GATA2, Gcg, GCLC, GHR, GIPR, GJA1, GRAP2, GSK3B, HADHA, HAND1, HBEGF, HDGF, HEXB, HEXIM1, HIC1, HIF1A, HK2, HLA-G, HPRT1, HSPA4, HSPA8, ICOSLG/LOC102723996, ID2, IFT122, IGFBP3, IGFBP4, IGFBP5, IL1RL1, IL7R, INHBA, ITGA1, ITGA5, ITGAV, ITGB5, JAK3, KEAP1, KIF1A, KRT19, LILRB3, LIPE, LMNA, LOXL2, LPAR2, LRP1, LTA, LTK, LUM, MAP1LC3A, MAP3K1, MAP3K2, MEF2D, MGP, MLH1, MMP14, MMP2, MMP9, MOAP1, MPL, MSH2, MSR1, MST1R, Mt3, MUS81, MUSK, MVP, NBN, NCSTN, NDEL1, NDNL2, NDST1, NEK4, NFATC4, NME3, NOS3, NOTCH2, NPC1, NR1D1, NR4A1, NRF1, NTF4, NUAK1, NUSAP1, OGT, OMA1, OSM, PAFAH1B1, PARL, PDCD1, PDCD11, PDCD6IP, PEG3, PFDN5, PHIP, PHLDA1, PIK3CB, PIN1, PLAT, PPP1R9A, PPP2R1A, PRKAG1, PRKG2, PROCR, PSAP, PTGS2, PTH1R, PTP4A2, PXN, RAB25, RAC3, RAPGEF3, RASSF6, RBBP6, REV3L, RGPD4 (includes others), RHOA, RHOB, RPRM, RPS6KB1, RXRA, S1PR3, SEMA7A, SERPINF1, SFT2D2, SH3GLB1, SHISA5, SIAH1, SIGIRR, SLC25A24, SLC46A2, SLIT3, SOCS3, SPI1, SPN, SPTLC2, SRC, SRCAP, ST14, ST3GAL1, STAMBP, STK38, STK4, STUB1, Tcf7, TFAP2C, TGFB1, THBD, THBS2, TIMP3, TNFAIP8L1, TNFSF13B, TNFSF14, TNRC6A, TRIB2, TRPM4, TTN, TWIST1, UBE2K, UBE2V1, UPF1, VAC14, VCL, VDR, VEGFB, VIPR1, WBP1, WISP1, YWHAZ, ZDHHC17, ZEB2, ZNF148, ZNF274, ZNF385A	271

Table 3.5 (cont'd).

	necrosis	4.33E-02	ABCB4, ABCE1, ADAM12, ADCYAP1, AGAP3, AGTR2, ANTXR2, ARF6, ARG1, ASTN1, ATF4, ATP6V1G2, ATR, B4GALNT1, BACE1, BCKDK, BCL2L1, BGN, BMP7, BMPR1A, BRCA1, CADPS2, CAMK2N2, CAMLG, CAPN1, CASP2, CAT, Ccl2, CD151, Cd24a, CD79B, CDH1, CDH5, CDKN1A, CFLAR, CHI3L1, CHRNA7, CIAPIN1, Clca3a1/Clca3a2, COL5A3, CPB2, CTF1, CTNNA1, CTSB, CUL7, CXADR, CXCL12, CYLD, CYP1B1, DDIT3, DDX58, DLL4, DMD, DNAJB1, DUSP1, E2F2, E2F4, EIF2AK1, EIF4EBP1, EMP2, EN2, FAAH, FABP1, FAM134B, FKBP4, FOSL1, GABBR1, GALNT3, GAS6, GATA2, Gcg, GHR, GIPR, GRAP2, GSK3B, HADHA, HBEGF, HDGF, HIF1A, HK2, HPRT1, HSPA8, ICOSLG/LOC102723996, ID2, IGFBP3, IGFBP4, IGFBP5, IL1RL1, IL7R, INHBA, ITGA1, ITGA5, JAK3, KEAP1, KIF1A, LILRB3, LIPE, LMNA, LPAR2, LRP1, LTA, LTK, MAP1LC3A, MAP3K1, MAP3K2, MEF2D, MLH1, MMP14, MMP2, MMP9, MPL, MSH2, MSR1, MST1R, Mt3, MUSK, MVP, NBN, NDEL1, NDNL2, NDST1, NEK4, NFATC4, NOS3, NPC1, NR1D1, NR4A1, NTF4, NUAK1, OGT, OMA1, OSM, PAFAH1B1, PARL, PDCD1, PDCD6IP, PEG3, PIK3CB, PIN1, PLAT, PPP1R9A, PROCR, PTGS2, PTH1R, PXN, RAB25, RAPGEF3, RGPD4 (includes others), RHOA, RHOB, RPRM, RPS6KB1, RXRA, S1PR3, SEMA7A, SERPINF1, SFT2D2, SH3GLB1, SIGIRR, SLC25A24, SLC46A2, SLIT3, SOCS3, SPI1, SPN, SPTLC2, SRC, SRCAP, ST14, ST3GAL1, STAMBP, STK38, STK4, STUB1, Tcf7, TFAP2C, TGFB1, THBD, THBS2, TIMP3, TNFAIP8L1, TNFSF13B, TRIB2, TRPM4, TTN, TWIST1, UBE2K, VAC14, VDR, WBP1, WISP1, YWHAZ, ZDHHC17, ZNF274	194
Cell Morphology	mineralization of cells	2.02E-02	ASPN, ATF4, BMP6, DKK2, GJA1, HEY1, HIVEP2, MGP, PTGS2, RHOA, SRC, TGFB1, TRPS1	13

Table 3.5 (cont'd).

Cell Morphology, Cellular Assembly and Organization	morphology of fibrils	2.02E-02	ADAMTS2, BGN, COL3A1, COL5A1, DSE, LUM, PLOD1, THBS2	8
	abnormal morphology of collagen fibrils	3.01E-02	ADAMTS2, BGN, COL3A1, COL5A1, DSE, PLOD1, THBS2	7
Cellular Movement	migration of cells	2.08E-03	ABCB4, ACTN4, ADAM12, ADAM33, ADCYAP1, ALOX5AP, ANGPT2, ANGPTL4, APBB1, APBB2, AQP1, ARAP3, ARF6, ASTN1, BGN, BMP6, BMPR1A, BRCA1, BSG, CADPS2, CAMK1, CAMK1D, CAT, CCL11, Ccl2, Ccl7, CCNA2, CD151, Cd24a, Cd59a, CD74, CD81, CDH1, CDH5, CDKN1A, CELSR1, CHI3L1, CHRNA7, CLEC7A, COL3A1, CPB2, CTNNA1, CTSB, CTTN, CXCL12, CYP1B1, CYP26A1, CYTIP, DAPK3, DDX58, DLL4, DOCK4, DOK1, DUSP1, Ear2 (includes others), EFNA5, EFS, EPB41L5, FAAH, FERMT3, FES, FHL2, FKBP4, FLRT2, FOSL1, FSCN1, FUT7, GAD1, GALNT1, GAS6, GBA, GJA1, GNA11, GPR124, GRB7, GSK3B, HBEGF, HDC, HIF1A, ICOSLG/LOC102723996, IGBP1, IGFBP4, IGFBP5, IL17B, IL1RL1, ITGA1, ITGA5, ITGA8, ITGAV, JAK3, KCNK2, KRT6B, LEFTY1, LILRB3, LMNA, LMNB1, LPAR2, LRP1, LTA, LTK, LUM, MAP2, MAP3K1, MAT1A, MATN2, MESP2, MINOS1-NBL1/NBL1, MMP13, MMP14, MMP2, MMP9, MRC2, MSR1, MST1R, NDEL1, NDST1, NOS3, NPC1, NR1D1, OCLN, OSM, PAFAH1B1, PDCD1, PF4, PGGT1B, PIK3CB, PLAT, PLET1, PLXND1, PPIC, PPM1A, PTGS2, PTX3, PXN, RAB27A, RAPGEF3, RASGRP4, RBFOX2, RGS16, RHOA, RHOB, RTN4, RXRA, S1PR3, SCHIP1, SDC2, SDC3, SNAI1, SOCS3, SPI1, SPN, SRC, STK4, TCIRG1, TFF2, TGFB1, THBD, THBS2, TIE1, TIMP3, TNFSF13B, TNFSF14, TNS1, TRAF4, TRPM4, TWIST1, VASP, VCL, VDR, WISP1, ZEB2	171

Table 3.5 (cont'd).

	cell movement	9.55E-03	ABCB4, ACTN4, ADAM12, ADAM33, ADCYAP1, ALOX5AP, ANGPT2, ANGPTL4, APBB1, APBB2, AQP1, ARAP3, ARF6, ASTN1, BGN, BMP6, BMPR1A, BRCA1, BSG, CADPS2, CAMK1, CAMK1D, CAPN1, CAT, CCL11, Ccl2, Ccl7, CCNA2, CD151, Cd24a, Cd59a, CD74, CD81, CDH1, CDH5, CDKN1A, Ceacam10, CELF3, CELSR1, CHDH, CHI3L1, CHRNA7, CLEC7A, COL3A1, CPB2, CTNNA1, CTSB, CTTN, CXCL12, CYP1B1, CYP26A1, CYTIP, DAPK3, DDHD1, DDX58, DLL4, DMD, DOCK4, DOK1, DUSP1, E2F2, Ear2 (includes others), EFNA5, EFS, EPB41L5, FAAH, FERMT3, FES, FHL2, FKBP4, FLRT2, FOSL1, FOSL2, FSCN1, FUT7, GAD1, GALNT1, GAS6, GBA, GJA1, GNA11, GPR124, GRB7, GSK3B, HAND1, HBEGF, HDC, HEXIM1, HIF1A, ICOSLG/LOC102723996, IGBP1, IGFBP3, IGFBP4, IGFBP5, IL17B, IL1RL1, ITGA1, ITGA5, ITGA8, ITGAV, JAK3, KCNK2, KRT6B, LEFTY1, LILRB3, LIPE, LMNA, LMNB1, LPAR2, LRP1, LTA, LTK, LUM, MAP2, MAP3K1, MAT1A, MATN2, MESP2, MINOS1-NBL1/NBL1, MMP13, MMP14, MMP2, MMP9, MRC2, MSR1, MST1R, NDEL1, NDST1, NOS3, NPC1, NR1D1, OCLN, OSM, PAFAH1B1, PDCD1, PF4, PGGT1B, PIK3CB, PLAT, PLET1, PLXND1, PPIC, PPM1A, PTGS2, PTX3, PXN, RAB27A, RAPGEF3, RASGRP4, RBFOX2, RGS16, RHOA, RHOB, RTN4, RXRA, S1PR3, SCHIP1, SDC2, SDC3, SNAI1, SOCS3, SPI1, SPN, SRC, STK4, TAS1R3, TCIRG1, TFF2, TGFB1, THBD, THBS2, TIE1, TIMP3, TNFSF13B, TNFSF14, Tnp1, TNS1, TRAF4, TRPM4, TWIST1, VASP, VCL, VDR, WISP1, ZEB2	185
Developmental Disorder	Growth Failure	2.35E-02	ACSS1, ACTN4, APEX1, AQP1, AQP2, ATF4, BACE1, BRCA1, C1GALT1C1, CDH5, CDKN1A, CFL2, CFLAR, COPS5, CRTAP, CTSB, CUL7, CYP11A1, DLD, DLL4, DPH1, E2F4, Elf5, FES, FKBP4, FOSL2, GALNT3, GCLC, GGT1, GHR, GPX2, Gulo, HADHA, HAP1, HEXA, HEXB, HIF1A, HK2, HOXC9, ID2, IP6K1, ITGA5, ITGAV, KRT6B, LMNA, LRP1, MGP, MMP14, MMP2, NBN, NCSTN, NFATC4, NOS3, NOTCH2, NTF4, OCLN, PARL, PCGF2, PDCD2, PIM3, PLAT, PLVAP, PROCR, PTH1R, PTS, RBBP6, RBMS1, REV3L, RPS6KB1, RXRA, SC5D, SCN1B, SHISA2, SLC11A2, SLC19A1, SMTN, SNAI1, SOX7, SPI1, SRC, STAMBP, STK4, SULF1, SYNE1, TCIRG1, TFAP2C, TFCP2L1, TGFB1, TIAL1, TTN, VCL, VDR, VIPR1, ZNF148	94

Table 3.5 (cont'd).

Developmental Disorder, Hereditary Disorder, Metabolic Disease	lysosomal storage disease	2.35E-02	Ccl2, GBA, GLB1, HEXA, HEXB, INSIG2, NOS3, NPC1, NPC2, PSAP, S1PR3	11
Digestive System Development and Function	abnormal morphology of digestive system	2.02E-02	ABCA5, ABCB4, ADAMTS2, AGTR2, ANGPTL4, APEX1, ARF6, ARG1, ATF4, BMP7, BRCA1, BSG, CADPS2, CDKN1A, CDON, CIAPIN1, CLEC7A, COL3A1, CTF1, CTHRC1, CYLD, DDX58, DNAJC3, DUSP1, E2F4, FAM20A, FES, FUT7, GAST, GDF1, GHR, GJA1, GRN, GSK3B, HADHA, HEXA, HEXB, HLX, ID2, IGFBP3, IGFBP4, IGFBP5, IL7R, INHBA, JAK3, KRT6B, LEFTY1, LOXL1, LTA, MAT1A, MMP14, NDST1, NFATC4, NOS3, NOTCH2, OCLN, PEX11A, PLVAP, PRKAG1, PSAP, PTGS2, PTH1R, PVRL3, RAPGEF3, RPS6KB1, RXRA, SC5D, SIAH1, SLC19A1, SLC22A4, SMTN, SOCS3, SOX7, SPI1, SRC, SULF1, TCIRG1, TFCP2L1, TFF2, TGFB1, TIE1, TIMP3, TMPO, TNFSF14, TRPS1, VDR, VIPR1	87
	morphology of digestive system	3.01E-02	ABCA5, ABCB4, ADAMTS2, AGTR2, ANGPTL4, APEX1, ARF6, ARG1, ATF4, BMP7, BRCA1, BSG, CADPS2, CDKN1A, CDON, CIAPIN1, CLEC7A, COL3A1, CTF1, CTHRC1, CYLD, DDX58, DNAJC3, DUSP1, E2F4, FAM20A, FES, FUT7, GAST, GDF1, GHR, GJA1, GRN, GSK3B, HADHA, HEXA, HEXB, HLX, ID2, IGFBP3, IGFBP4, IGFBP5, IL7R, INHBA, JAK3, KRT6B, LEFTY1, LOXL1, LTA, MAT1A, MMP14, NDST1, NFATC4, NOS3, NOTCH2, NTF4, OCLN, PEX11A, PLVAP, PRKAG1, PSAP, PTGS2, PTH1R, PTX3, PVRL3, RAPGEF3, RPS6KB1, RXRA, SC5D, SIAH1, SLC19A1, SLC22A4, SMTN, SOCS3, SOX7, SPI1, SRC, SULF1, TCIRG1, TFCP2L1, TFF2, TGFB1, TIE1, TIMP3, TMPO, TNFSF14, TRPS1, VDR, VIPR1	89
Lipid Metabolism, Molecular Transport, Small Molecule Biochemistry	accumulation of ganglioside GM2	1.08E-02	GLB1, HEXA, HEXB, NPC1, NPC2	5

Table 3.5 (cont'd).

	accumulation of glucosylceramide	2.02E-02	GBA, GLB1, NPC1, NPC2, PSAP	5
	accumulation of asialo GM2 ganglioside	3.01E-02	HEXA, HEXB, NPC1, NPC2	4
	accumulation of lactosylceramide	3.01E-02	GLB1, NPC1, NPC2, PSAP	4
Organismal Survival	organismal death	1.17E-02	ABCA5, ABCB4, ACSS1, ACTN4, ADAM12, ADCY3, ADCYAP1, AFF1, AGTR2, AKAP10, ANGPT2, ANGPTL4, ANTXR2, APBB1, APBB2, APEX1, AQP1, AQP2, ARAP3, ARF6, ARG1, ARHGDIB, ASNA1, ATF1, ATF4, ATP2A2, ATP8A2, ATR, B4GALNT1, BACE1, BACE2, BCL2L1, BGN, BICC1, BMP7, BMPR1A, BRCA1, BSG, C1GALT1C1, CADPS2, CAMLG, CAPN1, CARD10, CASP2, CBX4, CCL11, Ccl2, CCNA2, CD151, Cd59a, CD74, CDH1, CDH16, CDH5, CDK19, CDKN1A, CDON, CELSR1, CENPJ, CFL2, CFLAR, CHD8, CHRNA7, CIAPIN1, CLCF1, CLDN1, CLDN4, CLDN5, CLEC7A, CLUAP1, CNP, COL3A1, COL5A1, COPS5, CPB2, CPLX2, CRABP1, CRK, CSNK1A1, CSNK1D, CTSB, CTTN, CUL7, CXADR, CXCL12, CYLD, CYP11A1, CYP26A1, DDAH1, DDX58, DERL2, DISP1, DLD, DLL4, DMD, DNAJB9, DNAJC3, DNM3, DPH1, DSG2, DUSP1, E2F2, E2F4, ECM1, EFNA5, EIF2AK1, Elf5, ERCC8, FAM20A, FASN, FERMT3, FES, FKBP4, FLII, FLRT2, FLT4, FOSL1, FOSL2, FZD5, GABBR1, GABPA, GABPB1, GAD1, GALNT1, GAS6, GATA2, GBA, GBE1, GCLC,	316

Table 3.5 (cont'd).

Organismal Survival	organismal death	1.17E-02	GDF1, GGT1, GHR, GJA1, GNA11, GPR124, GPR4, GPX2, GRN, GSK3B, Gulo, HADHA, HAND1, HAP1, HBEGF, HEXA, HEXB, HEXIM1, HEY1, HIC1, HIF1A, HK2, HLX, HOXB3, HPRT1, HRH3, ID2, IDE, IDH1, IFT122, IGFBP5, Igtp, IL1RL1, INHBA, INSIG2, INTU, ITGA5, ITGA8, ITGAV, KCNK2, KEAP1, KIF1A, KPNA1, KRIT1, KRT19, KRT6B, LEFTY1, LIFR, LMNA, LMNB1, Lmo3, LRP1, LTA, MAB21L2, MAF, MAP2, MAP3K1, MASTL, MBTD1, MCM3AP, MEF2D, MESP2, MGP, MLH1, MLLT4, MMP14, MMP2, MMP9, MSH2, MSR1, MST1R, MUS81, MUSK, NAB1, NBN, NCSTN, NDEL1, NDST1, NFATC4, NFE2L3, NOS3, NOTCH2, NPC1, NRF1, NRXN1, NTF4, NUSAP1, OSM, PAFAH1B1, PARL, PCGF2, PDCD1, PDCD2, PEX11A, PIK3CB, PKNOX1, PLAT, PLOD1, PLVAP, PLXND1, PMM2, PPME1, PPP1R8, PPP1R9A, PROCR, PSAP, PSTPIP1, PTGS2, PTH1R, PTPRN, PTS, PTX3, PVRL3, PXN, RAB27A, RAC3, RAD54B, RASIP1, RBBP6, RBBP8, RBMS1, RBP2, REV3L, RFNG, RGPD4 (includes others), RHOA, RPS6KA4, RPS6KB1, RSPO1, RTN4, RXRA, S1PR3, SALL2, SC5D, SCN1B, SHANK3, SHISA2, SIAH1, SIGIRR, SLC11A2, SLC19A1, SLC22A4, SLC34A2, SMTN, SNAI1, SOCS3, SOX7, SPI1, SPTLC2, SRC, SRSF3, ST14, STAB1, STAMBP, STK4, STUB1, STX4, SULF1, SYNE1, Tcf7, TCIRG1, TFAP2C, TFCP2L1, TGFB1, TGS1, THBD, THBS2, TIAL1, TIE1, TIMP3, TNFSF13B, TRAF4, TRPS1, TTN, TWIST1, TWIST2, UPF1, VAC14, VASP, VCL, VDR, VEZT, VIPR1, ZEB2, ZNF148, ZNF274, ZNF385A	316

BIBLIOGRAPHY

BIBLIOGRAPHY

1. American Cancer Society: **Cancer Facts & Figures 2015**. Atlanta: American Cancer Society; 2015.

2. Howlader N, Noone A, Krapcho M, Garshell J, Miller D, Altekruse S, Kosary C, Yu M, Ruhl J, Tatalovich Z *et al* (eds.): **SEER Cancer Statistics Review, 1975-2012**. Bethesda, MD: National Cancer Institute; 2015.

3. Ziegler RG, Hoover RN, Pike MC, Hildesheim A, Nomura AM, West DW, Wu-Williams AH, Kolonel LN, Horn-Ross PL, Rosenthal JF *et al*: **Migration patterns and breast cancer risk in Asian-American women**. *J Natl Cancer Inst* 1993, **85**(22):1819-1827.

4. Stanford JL, Herrinton LJ, Schwartz SM, Weiss NS: **Breast cancer incidence in Asian migrants to the United States and their descendants**. *Epidemiology* 1995, **6**(2):181-183.

5. Hemminki K, Li X: **Cancer risks in Nordic immigrants and their offspring in Sweden**. *Eur J Cancer* 2002, **38**(18):2428-2434.

6. Beiki O, Hall P, Ekbom A, Moradi T: **Breast cancer incidence and case fatality among 4.7 million women in relation to social and ethnic background: a population-based cohort study**. *Breast Cancer Res* 2012, **14**(1):R5.

7. Mousavi SM, Fallah M, Sundquist K, Hemminki K: **Age- and time-dependent changes in cancer incidence among immigrants to Sweden: colorectal, lung, breast and prostate cancers**. *Int J Cancer* 2012, **131**(2):E122-128.

8. Andreeva VA, Unger JB, Pentz MA: **Breast cancer among immigrants: a systematic review and new research directions**. *J Immigr Minor Health* 2007, **9**(4):307-322.

9. Bassett MT, Levy L, Chokunonga E, Mauchaza B, Ferlay J, Parkin DM: **Cancer in the European population of Harare, Zimbabwe, 1990-1992**. *Int J Cancer* 1995, **63**(1):24-28.

10. Micozzi MS: **Nutrition, Body Size, and Breast Cancer**. *Yearbook of Physical Anthropology* 1985(28):175-206.

11. John EM, Phipps AI, Davis A, Koo J: **Migration history, acculturation, and breast cancer risk in Hispanic women**. *Cancer Epidemiol Biomarkers Prev* 2005, **14**(12):2905-2913.

12. Albuquerque RC, Baltar VT, Marchioni DM: **Breast cancer and dietary patterns: a systematic review**. *Nutr Rev* 2014, **72**(1):1-17.

13. World Cancer Research Fund / American Institute for Cancer Research: **Food, Nutrition, Physical Activity, and the Prevention of Breast Cancer**; 2010.

14. Brennan SF, Cantwell MM, Cardwell CR, Velentzis LS, Woodside JV: **Dietary patterns and breast cancer risk: a systematic review and meta-analysis**. *Am J Clin Nutr* 2010, **91**(5):1294-1302.

15. Thomson CA, Van Horn L, Caan BJ, Aragaki AK, Chlebowski RT, Manson JE, Rohan TE, Tinker LF, Kuller LH, Hou L *et al*: **Cancer incidence and mortality during the intervention and postintervention periods of the Women's Health Initiative dietary modification trial**. *Cancer Epidemiol Biomarkers Prev* 2014, **23**(12):2924-2935.

16. Sieri S, Chiodini P, Agnoli C, Pala V, Berrino F, Trichopoulou A, Benetou V, Vasilopoulou E, Sánchez M-J, Chirlaque M-D *et al*: **Dietary Fat Intake and Development of Specific Breast Cancer Subtypes**. *Journal of the National Cancer Institute* 2014, **106**(5).

17. Farvid MS, Cho E, Chen WY, Eliassen AH, Willett WC: **Adolescent meat intake and breast cancer risk**. *Int J Cancer* 2015, **136**(8):1909-1920.

18. Farvid MS, Cho E, Chen WY, Eliassen AH, Willett WC: **Dietary protein sources in early adulthood and breast cancer incidence: prospective cohort study**. *Bmj* 2014, **348**:g3437.

19. Farvid MS, Cho E, Chen WY, Eliassen AH, Willett WC: **Premenopausal dietary fat in relation to pre- and post-menopausal breast cancer**. *Breast Cancer Res Treat* 2014, **145**(1):255-265.

20. Renehan AG, Tyson M, Egger M, Heller RF, Zwahlen M: **Body-mass index and incidence of cancer: a systematic review and meta-analysis of prospective observational studies**. *Lancet* 2008, **371**(9612):569-578.

21. Inman JL, Robertson C, Mott JD, Bissell MJ: **Mammary gland development: cell fate specification, stem cells and the microenvironment**. *Development* 2015, **142**(6):1028-1042.

22. McDougall JA, Sakata R, Sugiyama H, Grant E, Davis S, Nishi N, Soda M, Shimizu Y, Tatsukawa Y, Kasagi F *et al*: **Timing of menarche and first birth in relation to risk of breast cancer in A-bomb survivors**. *Cancer Epidemiol Biomarkers Prev* 2010, **19**(7):1746-1754.

23. Medina D: **Mammary tumorigenesis in chemical carcinogen-treated mice. I. Incidence in BALB-c and C57BL mice**. *J Natl Cancer Inst* 1974, **53**(1):213-221.

24. Olson LK, Tan Y, Zhao Y, Aupperlee MD, Haslam SZ: **Pubertal exposure to high fat diet causes mouse strain-dependent alterations in mammary gland development and estrogen responsiveness**. *Int J Obes (Lond)* 2010, **34**(9):1415-1426.

25. Gahete MD, Cordoba-Chacon J, Lantvit DD, Ortega-Salas R, Sanchez-Sanchez R, Perez-Jimenez F, Lopez-Miranda J, Swanson SM, Castano JP, Luque RM *et al*: **Elevated GH/IGF-I promotes mammary tumors in high-fat, but not low-fat, fed mice**. *Carcinogenesis* 2014, **35**(11):2467-2473.

26. Zhao Y, Tan YS, Aupperlee MD, Langohr IM, Kirk EL, Troester MA, Schwartz RC, Haslam SZ: **Pubertal high fat diet: effects on mammary cancer development**. *Breast Cancer Res* 2013, **15**(5):R100.

27. Khalid S, Hwang D, Babichev Y, Kolli R, Altamentova S, Koren S, Goodwin PJ, Ennis M, Pollak M, Sonenberg N *et al*: **Evidence for a tumor promoting effect of high-fat diet independent of insulin resistance in HER2/Neu mammary carcinogenesis**. *Breast Cancer Res Treat* 2010, **122**(3):647-659.

28. Kim EJ, Choi MR, Park H, Kim M, Hong JE, Lee JY, Chun HS, Lee KW, Yoon Park JH: **Dietary fat increases solid tumor growth and metastasis of 4T1 murine mammary carcinoma cells and mortality in obesity-resistant BALB/c mice**. *Breast Cancer Res* 2011, **13**(4):R78.

29. Aupperlee MD, Zhao Y, Tan YS, Zhu Y, Langohr IM, Kirk EL, Pirone JR, Troester MA, Schwartz RC, Haslam SZ: **Puberty-specific promotion of mammary tumorigenesis by a high animal fat diet**. In: *Breast Cancer Res. Volume 17*, edn.; 2015.

30. Cleary MP, Grande JP, Juneja SC, Maihle NJ: **Diet-induced obesity and mammary tumor development in MMTV-neu female mice**. *Nutr Cancer* 2004, **50**(2):174-180.

31. Ford NA, Dunlap SM, Wheatley KE, Hursting SD: **Obesity, independent of p53 gene dosage, promotes mammary tumor progression and upregulates the p53 regulator microRNA-504**. *PLoS One* 2013, **8**(6):e68089.

32. Sundaram S, Freemerman AJ, Galanko JA, McNaughton KK, Bendt KM, Darr DB, Troester MA, Makowski L: **Obesity-mediated regulation of HGF/c-Met is associated with reduced basal-like breast cancer latency in parous mice**. *PLoS One* 2014, **9**(10):e111394.

33. Sundaram S, Freemerman AJ, Johnson AR, Milner JJ, McNaughton KK, Galanko JA, Bendt KM, Darr DB, Perou CM, Troester MA *et al*: **Role of HGF in obesity-associated tumorigenesis: C3(1)-TAg mice as a model for human basal-like breast cancer**. *Breast Cancer Res Treat* 2013, **142**(3):489-503.

34. Olivier M, Hainaut P: **TP53 mutation patterns in breast cancers: searching for clues of environmental carcinogenesis**. *Semin Cancer Biol* 2001, **11**(5):353-360.

35. Jerry DJ, Kittrell FS, Kuperwasser C, Laucirica R, Dickinson ES, Bonilla PJ, Butel JS, Medina D: **A mammary-specific model demonstrates the role of the p53 tumor suppressor gene in tumor development**. *Oncogene* 2000, **19**(8):1052-1058.

36. Mahabir S: **Association between diet during preadolescence and adolescence and risk for breast cancer during adulthood**. *J Adolesc Health* 2013, **52**(5 Suppl):S30-35.

37. Schrauwen P, Westerterp KR: **The role of high-fat diets and physical activity in the regulation of body weight**. *Br J Nutr* 2000, **84**(4):417-427.

38. Bandera EV, Chandran U, Hong CC, Troester MA, Bethea TN, Adams-Campbell LL, Haiman CA, Park SY, Olshan AF, Ambrosone CB *et al*: **Obesity, body fat distribution, and risk of breast cancer subtypes in African American women participating in the AMBER Consortium**. *Breast Cancer Res Treat* 2015, **150**(3):655-666.

39. Razzaghi H, Troester MA, Gierach GL, Olshan AF, Yankaskas BC, Millikan RC: **Mammographic density and breast cancer risk in White and African American Women**. *Breast Cancer Res Treat* 2012, **135**(2):571-580.

40. **Prevalence of Obesity Among Children and Adolescents: United States, Trends 1963-1965 Through 2009-2010**

41. Diamanti-Kandarakis E, Bourguignon JP, Giudice LC, Hauser R, Prins GS, Soto AM, Zoeller RT, Gore AC: **Endocrine-disrupting chemicals: an Endocrine Society scientific statement**. *Endocr Rev* 2009, **30**(4):293-342.

42. Jasik CB, Lustig RH: **Adolescent obesity and puberty: the "perfect storm"**. *Ann N Y Acad Sci* 2008, **1135**:265-279.

43. La Merrill M, Harper R, Birnbaum LS, Cardiff RD, Threadgill DW: **Maternal dioxin exposure combined with a diet high in fat increases mammary cancer incidence in mice**. *Environ Health Perspect* 2010, **118**(5):596-601.

44. Gu JW, Young E, Patterson SG, Makey KL, Wells J, Huang M, Tucker KB, Miele L: **Postmenopausal obesity promotes tumor angiogenesis and breast cancer progression in mice**. *Cancer Biol Ther* 2011, **11**(10):910-917.

45. Montgomery MK, Hallahan NL, Brown SH, Liu M, Mitchell TW, Cooney GJ, Turner N: **Mouse strain-dependent variation in obesity and glucose homeostasis in response to high-fat feeding**. *Diabetologia* 2013, **56**(5):1129-1139.

46. MR B, BG W, FK L, LR C: **Organ culture of whole mammary gland of the mouse**. *Tissue Culture Association Manual* 1976(2):457-462.

47. Aupperlee MD, Smith KT, Kariagina A, Haslam SZ: **Progesterone receptor isoforms A and B: temporal and spatial differences in expression during murine mammary gland development**. *Endocrinology* 2005, **146**(8):3577-3588.

48. Matsui Y, Halter SA, Holt JT, Hogan BL, Coffey RJ: **Development of mammary hyperplasia and neoplasia in MMTV-TGF alpha transgenic mice**. *Cell* 1990, **61**(6):1147-1155.

49. Cardiff RD, Anver MR, Gusterson BA, Hennighausen L, Jensen RA, Merino MJ, Rehm S, Russo J, Tavassoli FA, Wakefield LM *et al*: **The mammary pathology of genetically engineered mice: the consensus report and recommendations from the Annapolis meeting**. *Oncogene* 2000, **19**(8):968-988.

50. Allred DC, Harvey JM, Berardo M, Clark GM: **Prognostic and predictive factors in breast cancer by immunohistochemical analysis**. *Mod Pathol* 1998, **11**(2):155-168.

51. Herschkowitz JI, Simin K, Weigman VJ, Mikaelian I, Usary J, Hu Z, Rasmussen KE, Jones LP, Assefnia S, Chandrasekharan S *et al*: **Identification of conserved gene expression features between murine mammary carcinoma models and human breast tumors**. *Genome biology* 2007, **8**(5):R76.

52. McGuinness OP, Ayala JE, Laughlin MR, Wasserman DH: **NIH experiment in centralized mouse phenotyping: the Vanderbilt experience and recommendations for evaluating glucose homeostasis in the mouse**. *Am J Physiol Endocrinol Metab* 2009, **297**(4):E849-855.

53. Gouon-Evans V, Rothenberg ME, Pollard JW: **Postnatal mammary gland development requires macrophages and eosinophils**. *Development* 2000, **127**(11):2269-2282.

54. Cassetta L, Cassol E, Poli G: **Macrophage polarization in health and disease**. *ScientificWorldJournal* 2011, **11**:2391-2402.

55. Band H, Mirza S, Mohibi S, Band V: **Mouse models of estrogen receptor-positive breast cancer**, vol. 10; 2011.

56. Millikan RC, Newman B, Tse CK, Moorman PG, Conway K, Smith LV, Labbok MH, Geradts J, Bensen JT, Jackson S *et al*: **Epidemiology of basal-like breast cancer**. *Breast Cancer Res Treat* 2008, **109**(1):123-139.

57. Gyorffy B, Lanczky A, Eklund AC, Denkert C, Budczies J, Li Q, Szallasi Z: **An online survival analysis tool to rapidly assess the effect of 22,277 genes on breast cancer prognosis using microarray data of 1,809 patients**. *Breast Cancer Res Treat* 2010, **123**(3):725-731.

58. Alexandrow MG, Moses HL: **Transforming growth factor beta and cell cycle regulation**. *Cancer Res* 1995, **55**(7):1452-1457.

59. Kretzschmar M: **Transforming growth factor-beta and breast cancer: Transforming growth factor-beta/SMAD signaling defects and cancer**. *Breast Cancer Res* 2000, **2**(2):107-115.

60. Ten Dijke P, Goumans MJ, Itoh F, Itoh S: **Regulation of cell proliferation by Smad proteins**. *J Cell Physiol* 2002, **191**(1):1-16.

61. Kretzschmar M, Doody J, Timokhina I, Massagué J: **A mechanism of repression of TGFβ/ Smad signaling by oncogenic Ras**. *Genes Dev* 1999, **13**(7):804-816.

62. Riggins GJ, Kinzler KW, Vogelstein B, Thiagalingam S: **Frequency of Smad gene mutations in human cancers**. *Cancer Res* 1997, **57**(13):2578-2580.

63. Petersen M, Pardali E, van der Horst G, Cheung H, van den Hoogen C, van der Pluijm G, Ten Dijke P: **Smad2 and Smad3 have opposing roles in breast cancer bone metastasis by differentially affecting tumor angiogenesis**. *Oncogene* 2010, **29**(9):1351-1361.

64. Richly H, Aloia L, Di Croce L: **Roles of the Polycomb group proteins in stem cells and cancer**. *Cell Death Dis* 2011, **2**:e204.

65. Sauvageau M, Sauvageau G: **Polycomb Group Proteins: Multi-Faceted Regulators of Somatic Stem Cells and Cancer**. *Cell Stem Cell* 2010, **7**(3):299-313.

66. Tokimasa S, Ohta H, Sawada A, Matsuda Y, Kim JY, Nishiguchi S, Hara J, Takihara Y: **Lack of the Polycomb-group gene rae28 causes maturation**

arrest at the early B-cell developmental stage. *Exp Hematol* 2001, **29**(1):93-103.

67. Paul F, Pellegrini S, Uze G: **IFNA2: The prototypic human alpha interferon**. *Gene* 2015, **567**(2):132-137.

68. Trinchieri G: **Type I interferon: friend or foe?** *J Exp Med* 2010, **207**(10):2053-2063.

69. Chen BD, Najor F: **Macrophage activation by interferon alpha + beta is associated with a loss of proliferative capacity: role of interferon alpha + beta in the regulation of macrophage proliferation and function**. *Cell Immunol* 1987, **106**(2):343-354.

70. Swann JB, Hayakawa Y, Zerafa N, Sheehan KC, Scott B, Schreiber RD, Hertzog P, Smyth MJ: **Type I IFN contributes to NK cell homeostasis, activation, and antitumor function**. *J Immunol* 2007, **178**(12):7540-7549.

71. Nandi S: **Endocrine control of mammarygland development and function in the C3H/ He Crgl mouse**. *J Natl Cancer Inst* 1958, **21**(6):1039-1063.

72. Choi MS, Kim YJ, Kwon EY, Ryoo JY, Kim SR, Jung UJ: **High-fat diet decreases energy expenditure and expression of genes controlling lipid metabolism, mitochondrial function and skeletal system development in the adipose tissue, along with increased expression of extracellular matrix remodelling- and inflammation-related genes**. *Br J Nutr* 2015, **113**(6):867-877.

73. Martinez-Chacin RC, Keniry M, Dearth RK: **Analysis of high fat diet induced genes during mammary gland development: identifying role players in poor prognosis of breast cancer**. *BMC Res Notes* 2014, **7**:543.

74. La Merrill M, Baston DS, Denison MS, Birnbaum LS, Pomp D, Threadgill DW: **Mouse breast cancer model-dependent changes in metabolic syndrome-associated phenotypes caused by maternal dioxin exposure and dietary fat**. *Am J Physiol Endocrinol Metab* 2009, **296**(1):E203-210.

75. Murtaugh MA, Sweeney C, Giuliano AR, Herrick JS, Hines L, Byers T, Baumgartner KB, Slattery ML: **Diet patterns and breast cancer risk in Hispanic and non-Hispanic white women: the Four-Corners Breast Cancer Study**. *Am J Clin Nutr* 2008, **87**(4):978-984.

76. Smith-Warner SA, Spiegelman D, Adami HO, Beeson WL, van den Brandt PA, Folsom AR, Fraser GE, Freudenheim JL, Goldbohm RA, Graham S *et al*: **Types of dietary fat and breast cancer: a pooled analysis of cohort studies**. *Int J Cancer* 2001, **92**(5):767-774.

77. Boyd NF, Stone J, Vogt KN, Connelly BS, Martin LJ, Minkin S: **Dietary fat and breast cancer risk revisited: a meta-analysis of the published literature**. *Br J Cancer* 2003, **89**(9):1672-1685.

78. Alexander DD, Morimoto LM, Mink PJ, Lowe KA: **Summary and meta-analysis of prospective studies of animal fat intake and breast cancer**. *Nutr Res Rev* 2010, **23**(1):169-179.

79. Key TJ, Appleby PN, Cairns BJ, Luben R, Dahm CC, Akbaraly T, Brunner EJ, Burley V, Cade JE, Greenwood DC *et al*: **Dietary fat and breast cancer: comparison of results from food diaries and food-frequency questionnaires in the UK Dietary Cohort Consortium**. *Am J Clin Nutr* 2011, **94**(4):1043-1052.

80. Turner LB: **A meta-analysis of fat intake, reproduction, and breast cancer risk: an evolutionary perspective**. *Am J Hum Biol* 2011, **23**(5):601-608.

81. Berkey CS, Frazier AL, Gardner JD, Colditz GA: **Adolescence and breast carcinoma risk**. *Cancer* 1999, **85**(11):2400-2409.

82. Ruder EH, Dorgan JF, Kranz S, Kris-Etherton PM, Hartman TJ: **Examining breast cancer growth and lifestyle risk factors: early life, childhood, and adolescence**. *Clin Breast Cancer* 2008, **8**(4):334-342.

83. Linos E, Willett WC, Cho E, Frazier L: **Adolescent diet in relation to breast cancer risk among premenopausal women**. *Cancer Epidemiol Biomarkers Prev* 2010, **19**(3):689-696.

84. Medina D: **The mammary gland: a unique organ for the study of development and tumorigenesis**. *J Mammary Gland Biol Neoplasia* 1996, **1**(1):5-19.

85. Young LJT: **The Cleared Mammary Fat Pad and the Transplantation of Mammary Gland Morphological Structures and Cells**. In: *Methods in Mammary Gland Biology and Breast Cancer Research.* edn. Edited by Ip MM, Asch, Bonnie B: Springer Science & Business Media; 2000.

86. Kariagina A, Xie J, Langohr IM, Opreanu RC, Basson MD, Haslam SZ: **Progesterone stimulates proliferation and promotes cytoplasmic localization of the cell cycle inhibitor p27 in steroid receptor positive breast cancers**. *Horm Cancer* 2013, **4**(6):381-390.

87. Meyer G, Leipprandt J, Xie J, Aupperlee MD, Haslam SZ: **A potential role of progestin-induced laminin-5/alpha6-integrin signaling in the formation of side branches in the mammary gland**. *Endocrinology* 2012, **153**(10):4990-5001.

88. van Dierendonck JH, Wijsman JH, Keijzer R, van de Velde CJ, Cornelisse CJ: **Cell-cycle-related staining patterns of anti-proliferating cell nuclear antigen monoclonal antibodies. Comparison with BrdUrd labeling and Ki-67 staining**. *Am J Pathol* 1991, **138**(5):1165-1172.

89. Edgar R, Domrachev M, Lash AE: **Gene Expression Omnibus: NCBI gene expression and hybridization array data repository**. *Nucleic Acids Res* 2002, **30**(1):207-210.

90. Hanahan D, Weinberg RA: **Hallmarks of cancer: the next generation**. *Cell* 2011, **144**(5):646-674.

91. Coussens LM, Pollard JW: **Leukocytes in mammary development and cancer**. *Cold Spring Harb Perspect Biol* 2011, **3**(3).

92. Herschkowitz JI, Zhao W, Zhang M, Usary J, Murrow G, Edwards D, Knezevic J, Greene SB, Darr D, Troester MA *et al*: **Comparative oncogenomics identifies breast tumors enriched in functional tumor-initiating cells**. *Proc Natl Acad Sci U S A* 2012, **109**(8):2778-2783.

93. Prat A, Parker JS, Karginova O, Fan C, Livasy C, Herschkowitz JI, He X, Perou CM: **Phenotypic and molecular characterization of the claudin-low intrinsic subtype of breast cancer**. *Breast Cancer Res* 2010, **12**(5):R68.

94. Sabatier R, Finetti P, Guille A, Adelaide J, Chaffanet M, Viens P, Birnbaum D, Bertucci F: **Claudin-low breast cancers: clinical, pathological, molecular and prognostic characterization**. *Mol Cancer* 2014, **13**:228.

95. Lee YH, Rho YH, Choi SJ, Ji JD, Song GG: **The functional p53 codon 72 polymorphism is associated with systemic lupus erythematosus**. *Lupus* 2005, **14**(10):842-845.

96. Sanchez E, Sabio JM, Callejas JL, de Ramon E, de Haro M, Jimenez-Alonso J, Ortego-Centeno N, Sanchez-Roman J, Gonzalez-Gay MA, Lopez-Nevot MA *et al*: **Study of a functional polymorphism in the p53 gene in systemic lupus erythematosus: lack of replication in a Spanish population**. *Lupus* 2006, **15**(10):658-661.

97. Piotrowski P, Lianeri M, Mostowska M, Wudarski M, Chwalinska-Sadowska H, Jagodzinski PP: **Contribution of polymorphism in codon 72 of p53 gene to systemic lupus erythematosus in Poland**. *Lupus* 2008, **17**(2):148-151.

98. Onel KB, Huo D, Hastings D, Fryer-Biggs J, Crow MK, Onel K: **Lack of association of the TP53 Arg72Pro SNP and the MDM2 SNP309 with systemic lupus erythematosus in Caucasian, African American, and Asian children and adults**. *Lupus* 2009, **18**(1):61-66.

99. Chen RH, Chang CT, Wang TY, Huang WL, Tsai CH, Tsai FJ: **p53 codon 72 proline/arginine polymorphism and autoimmune thyroid diseases**. *J Clin Lab Anal* 2008, **22**(5):321-326.

100. Macchioni P, Nicoli D, Casali B, Catanoso M, Farnetti E, Boiardi L, Salvarani C: **The codon 72 polymorphic variants of p53 in Italian rheumatoid arthritis patients**. *Clin Exp Rheumatol* 2007, **25**(3):416-421.

101. Firestein GS, Echeverri F, Yeo M, Zvaifler NJ, Green DR: **Somatic mutations in the p53 tumor suppressor gene in rheumatoid arthritis synovium**. *Proc Natl Acad Sci U S A* 1997, **94**(20):10895-10900.

102. Han Z, Boyle DL, Shi Y, Green DR, Firestein GS: **Dominant-negative p53 mutations in rheumatoid arthritis**. *Arthritis Rheum* 1999, **42**(6):1088-1092.

103. Yamanishi Y, Boyle DL, Rosengren S, Green DR, Zvaifler NJ, Firestein GS: **Regional analysis of p53 mutations in rheumatoid arthritis synovium**. *Proc Natl Acad Sci U S A* 2002, **99**(15):10025-10030.

104. Inazuka M, Tahira T, Horiuchi T, Harashima S, Sawabe T, Kondo M, Miyahara H, Hayashi K: **Analysis of p53 tumour suppressor gene somatic mutations in rheumatoid arthritis synovium**. *Rheumatology (Oxford)* 2000, **39**(3):262-266.

105. Lin J, Huo R, Xiao L, Zhu X, Xie J, Sun S, He Y, Zhang J, Sun Y, Zhou Z *et al*: **A novel p53/microRNA-22/Cyr61 axis in synovial cells regulates inflammation in rheumatoid arthritis**. *Arthritis Rheumatol* 2014, **66**(1):49-59.

106. Rosenblum MD, Olasz E, Woodliff JE, Johnson BD, Konkol MC, Gerber KA, Orentas RJ, Sandford G, Truitt RL: **CD200 is a novel p53-target gene involved in apoptosis-associated immune tolerance**. *Blood* 2004, **103**(7):2691-2698.

107. Yoon KW, Byun S, Kwon E, Hwang SY, Chu K, Hiraki M, Jo SH, Weins A, Hakroush S, Cebulla A *et al*: **Control of signaling-mediated clearance of apoptotic cells by the tumor suppressor p53**. *Science* 2015, **349**(6247):1261669.

108. Maue AC, Yager EJ, Swain SL, Woodland DL, Blackman MA, Haynes L: **T-cell immunosenescence: lessons learned from mouse models of aging**. *Trends Immunol* 2009, **30**(7):301-305.

109. Haynes L, Maue AC: **Effects of aging on T cell function**. *Curr Opin Immunol* 2009, **21**(4):414-417.

110. Martin LJ, Li Q, Melnichouk O, Greenberg C, Minkin S, Hislop G, Boyd NF: **A randomized trial of dietary intervention for breast cancer prevention**. *Cancer Res* 2011, **71**(1):123-133.

111. Prentice RL, Caan B, Chlebowski RT, Patterson R, Kuller LH, Ockene JK, Margolis KL, Limacher MC, Manson JE, Parker LM *et al*: **Low-fat dietary pattern and risk of invasive breast cancer: the Women's Health Initiative Randomized Controlled Dietary Modification Trial**. *Jama* 2006, **295**(6):629-642.

112. Qian BZ, Pollard JW: **Macrophage diversity enhances tumor progression and metastasis**. *Cell* 2010, **141**(1):39-51.

113. Coussens LM, Werb Z: **Inflammation and cancer**. *Nature* 2002, **420**(6917):860-867.

114. Magne J, Mariotti F, Fischer R, Mathe V, Tome D, Huneau JF: **Early postprandial low-grade inflammation after high-fat meal in healthy rats: possible involvement of visceral adipose tissue**. *J Nutr Biochem* 2010, **21**(6):550-555.

115. Erridge C, Attina T, Spickett CM, Webb DJ: **A high-fat meal induces low-grade endotoxemia: evidence of a novel mechanism of postprandial inflammation**. *Am J Clin Nutr* 2007, **86**(5):1286-1292.

116. Suganami T, Tanimoto-Koyama K, Nishida J, Itoh M, Yuan X, Mizuarai S, Kotani H, Yamaoka S, Miyake K, Aoe S *et al*: **Role of the Toll-like receptor 4/NF-kappaB pathway in saturated fatty acid-induced inflammatory changes in the interaction between adipocytes and macrophages**. *Arterioscler Thromb Vasc Biol* 2007, **27**(1):84-91.

117. Renaud SC, Ruf JC, Petithory D: **The positional distribution of fatty acids in palm oil and lard influences their biologic effects in rats**. *J Nutr* 1995, **125**(2):229-237.

118. Boni-Schnetzler M, Boller S, Debray S, Bouzakri K, Meier DT, Prazak R, Kerr-Conte J, Pattou F, Ehses JA, Schuit FC *et al*: **Free fatty acids induce a proinflammatory response in islets via the abundantly expressed interleukin-1 receptor I**. *Endocrinology* 2009, **150**(12):5218-5229.

119. Dasu MR, Jialal I: **Free fatty acids in the presence of high glucose amplify monocyte inflammation via Toll-like receptors**. *Am J Physiol Endocrinol Metab* 2011, **300**(1):E145-154.

120. Rivera CA, Gaskin L, Singer G, Houghton J, Allman M: **Western diet enhances hepatic inflammation in mice exposed to cecal ligation and puncture**. *BMC Physiol* 2010, **10**:20.

121. Wang Z, Liu D, Wang F, Liu S, Zhao S, Ling EA, Hao A: **Saturated fatty acids activate microglia via Toll-like receptor 4/NF-kappaB signalling**. *Br J Nutr* 2012, **107**(2):229-241.

122. Villa-Osaba A, Gahete MD, Cordoba-Chacon J, de Lecea L, Pozo-Salas AI, Delgado-Lista FJ, Alvarez-Benito M, Lopez-Miranda J, Luque RM, Castano JP: **Obesity alters gene expression for GH/IGF-I axis in mouse mammary fat pads: differential role of cortistatin and somatostatin**. *PLoS One* 2015, **10**(3):e0120955.

123. Gwak JM, Jang MH, Kim DI, Seo AN, Park SY: **Prognostic value of tumor-associated macrophages according to histologic locations and hormone receptor status in breast cancer**. *PLoS One* 2015, **10**(4):e0125728.

124. Bhardwaj P, Du B, Zhou XK, Sue E, Harbus MD, Falcone DJ, Giri D, Hudis CA, Kopelovich L, Subbaramaiah K *et al*: **Caloric restriction reverses obesity-induced mammary gland inflammation in mice**. *Cancer Prev Res (Phila)* 2013, **6**(4):282-289.

125. Kim M, Cho HJ, Kwon GT, Kang YH, Kwon SH, Her S, Park T, Kim Y, Kee Y, Park JH: **Benzyl isothiocyanate suppresses high-fat diet-stimulated mammary tumor progression via the alteration of tumor microenvironments in obesity-resistant BALB/c mice**. *Mol Carcinog* 2015, **54**(1):72-82.

126. Colditz GA, Rosner BA, Chen WY, Holmes MD, Hankinson SE: **Risk factors for breast cancer according to estrogen and progesterone receptor status**. *J Natl Cancer Inst* 2004, **96**(3):218-228.